AD NUMBER
AD029109
CLASSIFICATION CHANGES
TO: unclassified
FROM: confidential
LIMITATION CHANGES
TO: Approved for public release, distribution unlimited
FROM: Distribution authorized to U.S. Gov't. agencies and their contractors; Foreign Government Information; NOV 1953. Other requests shall be referred to British Embassy, 3100 Massachusetts Avenue, NW, Washington, DC 20008.
AUTHORITY
DSTL, AVIA 28/3689, 17 Jul 2008; DSTL, AVIA 28/3689, 17 Jul 2008

CONFIDENTIAL

NOTICE: THIS DOCUMENT CONTAINS INFORMATION AFFECTING THE NATIONAL DEFENSE OF THE UNITED STATES WITHIN THE MEANING OF THE ESPIONAGE LAWS, TITLE 18, U.S.C., SECTIONS 793 and 794. THE TRANSMISSION OR THE REVELATION OF ITS CONTENTS IN ANY MANNER TO AN UNAUTHORIZED PERSON IS PROHIBITED BY LAW.

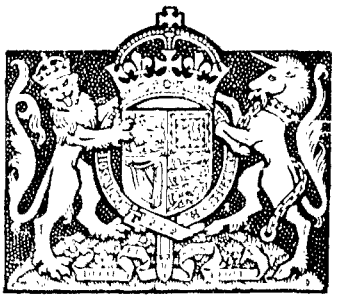

MINISTRY OF SUPPLY

NATIONAL GAS TURBINE ESTABLISHMENT
PYESTOCK, HANTS. WHETSTONE, LEICS.

REPORT No. R.143

THE COMPONENT PRESSURE LOSSES IN COMBUSTION CHAMBERS

by

H.A.KNIGHT and R.B.WALKER

NOVEMBER, 1953

Report No. R.143

November 1953

NATIONAL GAS TURBINE ESTABLISHMENT

The component pressure losses in combustion chambers

- by -

H. A. Knight and R. B. Walker

SUMMARY

This Report summarises the available knowledge of the component losses in a combustion chamber. The information given in this Report should enable the pressure drops through swirlers, primary baffles, cooling systems, etc., to be calculated. Most of the data were abstracted and collected from the various reports listed in the bibliography. In certain cases (e.g. mixing losses) the information is incomplete and in these circumstances the limited experimental results available are supplemented by hypotheses which require proof. A specimen calculation of the pressure drop and air flow distribution of a typical chamber is given in Appendix II. The calculated and measured values of pressure drop (cold) agreed within 4 per cent.

CONTENTS

CONTENTS (Cont'd.)

APPENDICES

ILLUSTRATIONS

1.0 Introduction

Effective combustion chamber design and development requires a knowledge of the air flow distribution throughout the chamber. Since the air flows through the chamber in two or three principal paths, arranged in parallel, the loss of total pressure in each path must be the same. Thus the division of air between the various paths will be determined by their relative resistances. This resistance to flow in each path is the summation of the individual component losses. For example, the primary circuit resistance comprises the swirler loss, diffusion loss, combustion loss, etc. Hence to obtain the air distribution in a given chamber the component losses must be calculable from design dimensions, and a method of combining the circuit resistances available. Such a method was developed by Probert and Kielland[1] and subsequently simplified[2] by dispensing with the "step-by-step" system of calculation. However, no comprehensive report on component losses has yet appeared although a note for discussion was published[3]. The present Report supplies the hitherto missing data much of which was obtained from unpublished work at N.G.T.E. In cases where the information is incomplete the available data are supplemented by hypotheses which require proof.

In the Report each component is considered in detail and the method of obtaining the overall loss and air distribution added for completeness. Appendix II gives a specimen calculation for a conventional chamber.

2.0 Swirlers

Flow conditions at outlet from a swirler vary along the blade span to satisfy radial equilibrium as shown in Appendix III. Thus, free vortex blading gives a constant axial velocity component while the whirl velocity varies inversely as the radius. Other forms of blading each have their own particular characteristics. Although true mean values of the velocity components should be used for pressure loss calculations, negligible error is involved and the tedium of obtaining these values obviated, by using values occurring at the weighted mean radius (r_m).

$$r_m = \frac{1}{\sqrt{2}} (R^2 + r_o^2)^{\frac{1}{2}} \qquad .. \quad .. \quad .. \quad .. \quad (1)$$

where the symbols have the significance given in Appendix I.

It is possible to study theoretically the efficiency of swirlers in turning the air through a given angle by considering the two dimensional flow of a perfect fluid through a lattice of plates. This problem has been studied[4] and the results applied[5] to connect the angle of deviation (α) with the pitch-chord ratio (σ) for various angles of stagger (β). In Figure 1 angle of deviation is plotted against pitch-chord ratio. The curves show that for quite practical pitch-chord ratios, i.e. $0.5 < \sigma < 1.0$ the deviation angle is almost identical with the stagger. Experimental results agree with this finding and it is now usual to employ pitch-chord ratios of about 0.7 for all swirlers required to give a tight swirl (i.e. high values of α and β). Thus for theoretical calculations on swirler pressure losses it is both convenient and justifiable to assume that the air is deviated through the entire stagger angle β.

2.1 Pressure drop due to a swirler

By considering in some detail the flow through the swirler and the resultant motion of the air, an expression for the pressure drop can be derived.

Consideration is now given to the outlet flow from the swirler at the mean radius as defined by Equation (1).

2.11 Whirl velocity component dissipated and constant static pressure

Dissipation of the whirl velocity head is the most obvious assumption regarding swirler pressure drops. But an assumption must then be made about the static pressure relationship at the swirler outlet (1) and at a plane (2) situated downstream in the flame tube. A likely assumption is that the mean static pressure difference is negligible.

A mere statement of the total pressure loss is obtained by applying Berroullis equation, thus

$$P_1 = P_2 + \text{loss} \qquad .. \quad .. \quad .. \quad .. \quad .. \quad .. \quad .. \quad (2)$$

with the further assumption of constant static pressure this reduces to

$$\text{loss} = P_1 - P_2 = \frac{1}{2}\rho(V_1^2 - V_2^2) \qquad .. \quad .. \quad .. \quad .. \quad .. \quad (3)$$

and since

$$V_1 = V_a \sec \alpha$$

$$V_2 = V_a \frac{A_s}{A_F} \quad \text{(whirl component lost)}$$

$$\text{loss} = \frac{1}{2}\rho V_a^2 \left\{ \sec^2 \alpha - \left(\frac{A_s}{A_F}\right)^2 \right\} \qquad .. \quad .. \quad .. \quad .. \quad (4)$$

$$\therefore \quad \Phi_F = \left\{ \left(\frac{A_F}{A_s}\right)^2 \sec^2 \alpha - 1 \right\} \qquad .. \quad .. \quad .. \quad .. \quad (5)$$

2.12 Whirl velocity component dissipated and axial momentum conserved

A more logical assumption than constant static pressure is conservation of axial momentum. Even this must have certain limitations since the axial momentum is unevenly distributed across the flame tube diameter and is negative along the axis due to flow reversal.

The momentum equation is

$$P_1 A_s - P_2 A_F + \left(\frac{P_1 + P_2}{2}\right)\left(A_F - A_s\right) = \rho A_s V_a^2 \left\{\frac{A_s}{A_F} - 1\right\} \quad .. \quad .. \quad .. \quad .. \quad (6)$$

$$\text{thus} \quad P_1 - P_2 = 2\left(\frac{A_s}{A_F}\right)\left(\frac{A_s - A_F}{A_s + A_F}\right)\rho V_a^2$$

$$\text{and} \quad \Phi_F = \left(\frac{A_F}{A_s}\right)^2 \sec^2 \alpha - 1 + 4\left(\frac{A_F}{A_s}\right)\left(\frac{A_s - A_F}{A_s + A_F}\right)$$

$$.. \quad .. \quad .. \quad .. \quad (7)$$

2.13 Consideration of most reliable assumption

Of these two views the former has proved to be the more reliable. Although there is the possibility of some slight pressure recovery by virtue of the area change it is undoubtedly local and is dissipated by the friction in the ensuing recirculation and general combustion turbulence. The comparison is good between measured losses given in Reference 5 and by calculation using Equation (12) which is Equation (5) plus the blade loss. For typical values of A_F, A_s and α the difference in loss factor Φ_F by using Equations (5) and (7) rarely exceeds 5 per cent, the former giving better agreement with experimental results. Conservation of axial and angular momentum considerably increases the difference between calculated and experimental results.

2.14 Blade losses

In the foregoing analysis the losses are assumed to originate from the resultant flow conditions of the air after leaving the swirler and no mention was made of the losses in the swirler itself. These are due to profile and secondary losses in the blades. The former are losses attributable to skin friction and separation, the latter due to three dimensional effects. These losses are approximately of the same magnitude and in the case of swirlers where the incidence is zero, the principal factors affecting the overall blade loss are outlet angle, pitch-chord ratio and blade passage area. However, since the blade loss represents a very small proportion of the total swirler loss, an average figure of 15 per cent of the

swirler outlet velocity head is taken[6] for the blade loss for values of (α) in the range $65^\circ < \alpha < 85^\circ$. This figure was experimentally determined (see Reference 6) and is independent of blade form.

For smaller values of (α) and for increased accuracy where such variables as blade height and thickness are taken into account, the following method abstracted from Reference 7 is used.

This method is used for determining the losses in turbine nozzle guide vanes and there are obvious limitations when it is applied to swirlers. Errors are most likely to be associated with the secondary loss coefficient. Hub ratios $\left(\frac{d}{D}\right)$ for turbines are of the order 0.8 whereas for swirlers they are about 0.2. Reducing the hub ratio undoubtedly increases the secondary loss for turbines and will presumably affect swirlers similarly, although to a greater degree. However, the deflection angles and flow accelerations are higher in swirlers and the latter at least will tend to reduce the loss. These various effects are allowed for (see Section (b) below), but the overall impression is that the method of Reference 8 when applied to swirlers tends to underestimate the secondary loss. Unfortunately there are not sufficient swirler tests for an independent estimate of the secondary loss to be made.

Conditions are considered at the reference radius r_m.

Details required (see Appendix I and Figure 2).

(1) Blade chord - c at reference radius

(2) Blade pitch - s at reference radius

Blade thickness ~ t - at reference radius

Free swirler area ~ $A_s = \Pi(R^2 - r_o^2)$

(a) Profile loss coefficient

From Figure 3 knowing (α) and the pitch-chord ratio (σ) the profile loss coefficient (Y_p) is obtained.

(b) Secondary loss coefficient

For zero incidence and assuming $\alpha = \beta$

$$\tan \alpha_n = \frac{1}{2} \tan \alpha \quad .. \quad .. \quad .. \quad .. \quad (8)$$

$$\text{also } C_L/(s/c) = 2 \tan \alpha \cdot \cos \alpha_n \quad .. \quad .. \quad (9)$$

The secondary loss for zero incidence

$$Y_s = K\left[C_L/(s/c)\right]^2 \left[\cos^2\alpha/\cos^3\alpha_n\right] \quad .. \quad .. \quad .. \quad .. \quad (10)$$

The factor K is a function of $\dfrac{(A_t/A_s)^2}{\left[1 + \frac{d}{D}\right]}$ and is plotted in Figure 4.

$$A_s = \Pi (R^2 - r_o^2)$$

$$A_t = A_n \cos \alpha \quad (A_n = \text{swirler outlet area})$$

(c) Total loss coefficient (Y_t)

$$Y_t = Y_p + Y_s \qquad .. \quad .. \quad .. \quad .. \quad .. \quad .. \quad (11)$$

If the t/s (thickness/pitch) ratio differs from 0.02 then the total loss coefficient should be corrected by the multiplication factor given in Figure 5.

2.15 Effect of Reynolds number on blade losses

The Reynolds number for a swirler is defined in the usual manner using the blade chord as the scalar length and the outlet absolute velocity, density and viscosity at the mean radius r_m. For all forms of aerodynamic machine the loss increases with decrease of Reynolds number especially in the range $Re < 10^5$. The effect of Reynolds number on profile loss may be determined approximately from Figure 6 which has relative loss coefficient (defined as $\frac{Y_p}{Y_p \text{ at } Re = 2 \times 10^5}$) plotted against Re and is for all forms of blading. The secondary losses are assumed to be independent of Reynolds number[8].

2.16 Overall loss coefficient for a swirler

From Equation (7) and Section 2.14 the total loss coefficient for the swirler in terms of the flame tube area A_F.

$$\Phi_F = 1.15 \left(\frac{A_F}{A_s}\right)^2 \sec^2 \alpha - 1 \qquad .. \quad .. \quad .. \quad .. \quad (12)$$

or a little more accurately

$$\Phi_F = \left(\frac{A_F}{A_s}\right)^2 \sec^2 \alpha \left\{1 + Y_t\right\} - 1 \quad .. \quad .. \quad .. \quad .. \quad (13)$$

2.17 Overall loss coefficient for various types of swirler

Equations (12) and (13) are quite general equations for conventional swirlers and it only remains for one or two general observations to be made when these formulae are applied to the various types of swirler.

2.18 Constant blade angle - curved blades

This type of swirler is frequently used where 'tight' swirls are required and where the velocities are relatively high. The blades are curved so that the upstream edges are parallel to the flow, i.e. zero incidence.

Either Equations (12) or (13) may be used to determine the loss factor (Φ_F).

2.19 Constant blade angle - straight blades

This type of swirler is very easily manufactured and is representative of the swirlers used in large industrial type chambers, where the overall velocities are low. Since the incidence of the blades is extremely high, the loss factor is also very high, although the flat blades are extremely effective in deviating the air through the required angle. Scanty evidence[5] suggests that the blade loss is approximately doubled compared with curved blades for the same value of (α) where $65^\circ < \alpha < 85^\circ$.

Hence loss coefficient for swirler with flat plates is given by

$$\Phi_F = 1.3 \left(\frac{A_F}{A_s}\right)^2 \sec^2 \alpha - 1 \qquad .. \quad .. \quad .. \quad .. \quad .. \quad .. \quad (14)$$

Obviously, the more accurate calculation of Y_t is impossible in this instance since the blades are permanently stalled due to the very high incidence.

2.20 Varying blade angle - curved blades

In view of the manufacturing difficulties and the small increase in performance over the constant blade angle type, this type of swirler is now rarely used. The blades are usually of free vortex form giving maximum whirl velocity and hence low pressure at the centre. To apply the loss coefficient formula it is necessary to ascribe a value to ($\sec \alpha$). As mentioned in Section 2.0 negligible error is involved by applying values occurring at the mean radius (r_m). As shown in Appendix III if the blades are of free vortex form (V_a) is constant and

$$\sec^2 \alpha = 1 + \frac{2 r_o^2}{R^2 + r_o^2} \tan^2 \alpha_o$$

$$\text{and } \Phi_F = \left[\left(\frac{A_F}{A_s}\right)^2 \left(1 + \frac{2 r_o^2}{R^2 + r_o^2} \tan^2 \alpha_o\right)\left(1 + Y_t\right)\right] - 1 \qquad .. \quad .. \quad (15)$$

For forced vortex blades (rarely used)

$$\sec^2 \alpha = 1 + \frac{R^2 + r_o^2}{2(r_o^2 \operatorname{cosec}^2 \alpha_o - R^2)}$$

$$\text{and } \Phi_F = \left[\left(\frac{A_F}{A_s}\right)^2 \left\{1 + \frac{R^2 + r_o^2}{2(r_o^2 \operatorname{cosec}^2 \alpha_o - R^2}\right\}(1 + Y_t)\right] - 1 \qquad .. \quad (16)$$

2.21 Ported swirler (Figure 7)

The development of a combustion chamber having low wall temperatures resulted in a stabilising baffle embodying this type of swirler. Assuming no pressure recovery and the static pressure difference between the swirler outlet and flame tube are negligible, as in Section 2.13;

$$\text{loss} = \tfrac{1}{2}\rho\,(V_1^2 - V_2^2)$$

From the velocity triangle of Figure 7

$$V_1 = V_a' \operatorname{cosec}\alpha$$

$$V_a = V_a' \sin\theta$$

$$V_2 = V_a \frac{A_s}{A_F}$$

$$\therefore \quad \text{loss} = \tfrac{1}{2}\rho\, V_a^2 \left\{ \operatorname{cosec}^2\theta \operatorname{cosec}^2\alpha - \left(\frac{A_s}{A_F}\right)^2 \right\}$$

$$\therefore \quad \Phi_F = \left\{ \left(\frac{A_F}{A_s}\right)^2 \operatorname{cosec}^2\theta \ \operatorname{cosec}^2\alpha \right\} - 1 \quad .. \quad .. \quad .. \quad .. \quad (17)$$

From Equation (17), as the semi-angle of the cone and the air angle through the ports relative to the tangent at the ports increase, the loss decreases. This is to be expected. There are no known experimental results from which an allowance for blade loss, i.e. air friction at the ports, can be made.

2.22 Tangential port swirler

This type of swirler was last used on the early types of chamber for the W2B, W2/500 and W2/700 engines, and may not be used in the same form again. For the purpose of determining the loss it is reasonable to assume that the velocity head through the ports is lost.

$$\text{i.e.} \quad \Phi_F = \left(\frac{A_F}{A_s}\right)^2 \quad .. \quad .. \quad .. \quad .. \quad .. \quad .. \quad .. \quad .. \quad (18)$$

2.23 Vortex type swirler (Figure 8)

This type of swirler is basically a small vortex chamber followed by a throat and is a comparatively new type. Its ability to 'run full' gives it an advantage over the conventional swirler. With reference to Figure 8, the pressure loss comprises two principal components. Firstly, that due to

producing the whirl velocity at the throat and secondly, the production of the axial velocity component.

The pressure drop between the tangential entry and the throat is mainly a friction drop and assuming the vortex decay law

$$V_w r^n = c$$

Total pressure drop ΔP can be shown to be

$$\Delta P = \frac{\rho c^2}{2}\left\{\left(\frac{1}{r_2}\right)^{2n} - \left(\frac{1}{r_1}\right)^{2n}\right\}\left\{\frac{1}{n} - 1\right\} \quad .. \quad .. \quad .. \quad .. \quad .. \quad .. \quad (19)$$

by integrating the equation for static pressure drop in vortex flow:

$$\frac{dp}{dr} = \rho \frac{V_w^2}{r}$$

between r_1 and r_2 and since the swirl energy at the throat is irrecoverable

$$\Delta P = \frac{\rho c^2}{2}\left\{\left(\frac{1}{r_2}\right)^{2n} - \left(\frac{1}{r_1}\right)^{2n}\right\}\left\{\frac{1}{n} - 1\right\} + \frac{1}{2}\rho V_{w_2}^2$$

and also the axial outlet velocity must be produced.

Hence total pressure drop

$$\Delta P = \frac{\rho c^2}{2}\left\{\left(\frac{1}{r_2}\right)^{2n} - \left(\frac{1}{r_1}\right)^{2n}\right\}\left\{\frac{1}{n} - 1\right\} + \frac{1}{2}\rho V_{w_2}^2 + \frac{1}{2}\rho V_a^2\left\{1 - \left(\frac{A_t}{A_F}\right)^2\right\}$$

also by continuity $V_{w_1} A_s = A_t V_a = A_F V_F \quad .. \quad .. \quad .. \quad .. \quad .. \quad (20)$

$$\therefore \Delta P = \frac{\rho V_{w_1}^2}{2}\left[\left(\frac{r_1}{r_2}\right)^{2n}\frac{1}{n} - \left(\frac{1}{n} - 1\right) + \left(\frac{A_s}{A_t}\right)^2\left\{1 - \left(\frac{A_t}{A_F}\right)^2\right\}\right] \quad .. \quad .. \quad .. \quad (21)$$

thus

$$\Phi_F = \left(\frac{A_F}{A_s}\right)^2\left[\left(\frac{r_1}{r_2}\right)^{2n}\frac{1}{n} - \left(\frac{1}{n} - 1\right) + \left(\frac{A_s}{A_t}\right)^2\left\{1 - \left(\frac{A_t}{A_F}\right)^2\right\}\right] \quad .. \quad .. \quad .. \quad (22)$$

For a free vortex n = 1, but tests on a model cyclone of approximately 18 in. maximum diameter and 6 in. wide have shown n = 0.95, and that n decreases further as the width is reduced. Since for a practical size of swirler the effective Reynolds number is lower and the flow area/wetted area ratio is greater, n will probably be of the order 0.8. No experimental results are available for confirmation of this value. The angle of swirl at the throat (ω) is given by

$$\omega = \tan^{-1} \frac{V_{w_2}}{V_a}$$

$$\text{i.e.} \quad \tan \omega = \left(\frac{r_1}{r_2}\right)^n \frac{A_t}{A_s} \qquad .. \quad .. \quad .. \quad .. \quad .. \quad (23)$$

Thus a wide latitude is allowed in designing a vortex swirler for a given value of swirl angle.

2.3 Swirler followed by a throat

The combination of a swirler followed by a throat occurs frequently in chambers containing ceramic liners. This problem was studied [9] and predicted values for the pressure loss were closely substantiated by experimental results. The problem is complicated by the fact that heat addition occurs at the reference planes downstream from the swirler exit. With reference to the notational diagram Figure 9

$$\text{Axial velocity from swirler outlet} = \frac{A_F}{A_s} \cdot \frac{\rho'}{\rho} \cdot V_F \qquad .. \quad .. \quad .. \quad .. \quad (24)$$

$$\text{Whirl velocity from swirler outlet} = \frac{A_F}{A_s} \cdot \frac{\rho'}{\rho} V_F \tan \alpha \qquad .. \quad .. \quad .. \quad .. \quad (25)$$

The kinetic energy changes between the plane of the swirler outlet and the ceramic liner throat are based on the assumptions that the axial velocity component increases in the ratio of the areas and the whirl velocity in the square root of this ratio, making it a type of free vortex. This latter assumption implies that the moment of momentum is constant on a stream surface and is described in Reference 5.

$$\text{Axial velocity at throat} = \frac{A_F}{A_t} \cdot V_F \cdot \frac{\rho'}{\rho''} \qquad .. \quad .. \quad .. \quad .. \quad (26)$$

$$\text{Whirl velocity at throat} = \frac{A_F}{A_s} \cdot \sqrt{\frac{A_s}{A_t}} \frac{\rho'}{\rho''} \cdot V_F \tan \alpha \qquad .. \quad .. \quad .. \quad (27)$$

Thus assuming no pressure recovery and the static pressure difference to be negligible between the throat and the flame tube downstream

$$\text{loss} = \frac{1}{2}\rho'' V_t^2 - \frac{1}{2}\rho' V_F^2$$

$$= \frac{1}{2}\rho'' \left\{ \left(\frac{\rho'}{\rho''}\right)^2 \left(\frac{A_F}{A_s}\right)^2 \cdot \frac{A_s}{A_t} \cdot V_F^2 \tan^2\alpha + \left(\frac{A_F}{A_t}\right)^2 \cdot V_F^2 \left(\frac{\rho'}{\rho''}\right)^2 \right\} - \frac{1}{2}\rho' V_F^2$$

$$= \frac{1}{2}\rho' V_F^2 \left[\frac{\rho'}{\rho''} \left\{ \left(\frac{A_F^2}{A_s A_t}\right) \tan^2\alpha + \left(\frac{A_F}{A_t}\right)^2 \right\} - 1 \right] \quad .. \quad .. \quad .. \quad (28)$$

the blade loss in the swirler is

$$Y_t \left\{ \frac{1}{2}\rho \left(\frac{A_F}{A_s} \cdot \frac{\rho'}{\rho} V_F \sec\alpha \right)^2 \right\} \quad .. \quad .. \quad .. \quad (29)$$

Overall loss factor obtained by combining Equations (28) and (29) and simplifying

$$\Phi_F = \left[\left(\frac{\rho'}{\rho''}\right) \left(\frac{A_F}{A_t}\right)^2 \left\{ \frac{A_t}{A_s} \tan^2\alpha + 1 \right\} + Y_t \left(\frac{\rho'}{\rho}\right) \left(\frac{A_F}{A_s}\right)^2 \sec^2\alpha \right] - 1$$

$$.. \quad .. \quad .. \quad .. \quad (30)$$

In Equation (30) Y_t is determined by the methods given in Sections 2.14, 2.15 and 2.19.

In the design or project stage, it is difficult to ascribe values to ρ'' i.e. the density at the throat. However, the density relationship throughout the primary zone may be written:-

$$\left(\frac{1}{\rho''} - \frac{1}{\rho}\right) = G\left(\frac{1}{\rho'} - \frac{1}{\rho}\right) \quad .. \quad .. \quad .. \quad .. \quad .. \quad .. \quad .. \quad .. \quad .. \quad (31)$$

which is based on a temperature relationship assuming constant static pressure. G is a factor ($0 < G < 1$) depending upon the amount of heat release between the exit of the swirler and the throat. The value of $\frac{\rho}{\rho'} = x$ say,

can usually be fixed with a reasonable accuracy, and Equation (31) reduces to

$$\frac{\rho''}{\rho} = \frac{1}{G\,(x - 1) + 1} \qquad .. \quad .. \quad .. \quad .. \quad .. \quad (32)$$

By substituting probable values for G, ρ'' is obtained. In practice it is doubtful if G will exceed 0.5 and generally $0.25 < G < 0.5$. In the previous analysis[9] taking values of G of 0.25 and 0.5 varied the primary loss factor some 30 per cent and the overall loss factor some 7 per cent. Thus the value ascribed to G is not really critical in determining the overall loss of the chamber.

3.0 Primary stabiliser losses

The fundamental principle of flame stabilisation is to reduce the local velocity and effect a flow reversal by which fresh mixture is added to the piloting region to propagate combustion. This is achieved by two distinct forms of piloting system, viz. gutter and plain baffle type stabilisers. The former type are used where high velocity conditions exist i.e. ram jets, reheat etc., and although considerable work is being carried out on gutters few published notes are available. The plain baffle type stabilisers incorporating a swirler are used in the majority of aero engine and industrial type chambers.

3.1 Plain baffles

These plain baffles are of varying form although they do preserve some symmetry in design. To obtain the complete baffle loss the pressure loss of the various free area shapes (holes, scoops, etc.), which constitute the baffle must be determined. When air flows through these various holes the issuing free jets are conoidal in shape and hence give rise to a discharge coefficient. If C_{d_o} and A_o are the overall discharge coefficient and total free area of the baffle respectively and the various components have free areas A_1, A_2, A_3 ..... and discharge coefficients C_{d_1}, C_{d_2}, C_{d_3} .....

then
$$C_{d_o} = \frac{A_1 C_{d_1} + A_2 C_{d_2} + A_3 C_{d_3} .....}{A_1 + A_2 + A_3 .....}$$

$$= \frac{\Sigma\, A\, C_d}{\Sigma\, A} \qquad .. \quad .. \quad .. \quad .. \quad .. \quad .. \quad .. \quad (33)$$

Thus any shape or size of baffle can be reduced to the simple case of an equivalent hole in a flat plate. The necessary experimental values of discharge coefficient are taken from experimental results obtained at N.G.T.E. and will be published[10] in collected form shortly. Briefly, the various baffles were mounted in a test section and the loss of total pressure measured for a range of velocities. Theoretically[11], the pressure loss is calculable providing the free area of the baffle, the cross-sectional area

to which the flow expands (in terms of area, since this is actually a diffusion process) and the discharge coefficient are known. The former values are obtained by actual measurement but the discharge coefficient can only be determined experimentally.

3.2 Variables affecting the pressure loss of plain baffles

3.21 Effect of velocity

The theoretical curves[11] show that the non-dimensional loss factor increases with Mach number which for constant static temperature is proportional to the velocity. Pressure loss tests on various baffle shapes have shown that the loss does in fact increase with Mach number but at a reduced rate of increase to that predicted. It was thought that an increase in the discharge coefficient with Mach number might account for the discrepancy and this has now been substantiated by independent experiments[12]. Variation of (C_d) with vena-contracta Mach number is shown in Figure 10. For most combustion chambers the change of C_d is small, but since the loss is inversely proportional to C_d^2 its effect will be significant.

3.22 Effect of area ratio

For a given shape of hole the discharge coefficient increases initially almost as the square of the area ratio as shown in Figure 11 in which the relative coefficient is plotted against area ratio. This curve is based on values obtained from Reference 13 and by experiment and is for sharp edged circular orifices. The equivalent curve for other shapes of orifice will be slightly different.

3.23 Effect of hole size

The effect of using baffles containing a similar total area of holes of different size has not resulted in any definite conclusions being reached. A large number of small holes would be expected to give a higher loss on account of the larger wetted area available for friction. However, experimental results show the converse to be true, i.e. the baffle having a small number of large holes has a 2 per cent higher pressure loss. It should be appreciated that the experimental error is of this order and also variation in the diameter of the holes has to be extremely small to account for this difference.

3.24 Effect of hole shape

The shape of the hole for a given free area does affect the pressure loss by variation in the discharge coefficient. Circular holes have the lowest discharge coefficient for a given free area. Square orifices have slightly higher values of C_d and rectangular and elliptical orifices with high values of major/minor axis ratio higher values still. Typical minimum values i.e. corresponding to infinite area ratio, are given in Table I below.

TABLE I

Type	Circular	Square	Rectangular	Elliptical	Elliptical
Axis ratio	-	1	3:1	2:1	4:1
C_d	0.60	0.62	0.63	0.62	0.63
Hydraulic mean depth	$0.282\sqrt{A}$	$0.25\sqrt{A}$	$0.214\sqrt{A}$	$0.26\sqrt{A}$	$0.204\sqrt{A}$

The vena-contracta is formed by the inward radial flows on the upstream face of the baffle acting on the jet periphery. For a hole in the centre of the baffle these contracting forces are strongest when acting normal to the jet surface. For a circular hole the forces act normal to the surface over the entire periphery and produce the greatest contraction. Thus contraction coefficient (C_c) increases as the hole shapes become "less circular", i.e. elliptical (2:1), square, rectangular, etc.

(C_v), velocity coefficient, represents the ratio of actual to theoretical velocity through the hole and is due to viscosity and boundary friction. Hence increasing the periphery of a hole for a given cross-sectional area results in a decrease of (C_v). For holes in thin plates C_v tends to unity and as periphery variations (as shown in Table I where hydraulic mean depth = $\frac{\text{cross sectional area}}{\text{periphery}}$) are small, changes in (C_v) are negligible. Since discharge coefficient = $C_d = C_c \cdot C_v$ changes in C_c will be the predominating factor. Thus for maximum discharge through a given area the hole shape should be rectangular with, for example, an axis ratio of 4:1. However, practical disadvantages such as corner stress concentrations and manufacturing difficulties may outweigh the advantage of the small increase in (C_d).

For an annulus around a hemispherical baffle mean values of 0.9 for the discharge coefficient were obtained.

"Thumbnail" scoops have a discharge coefficient closely approaching unity.

3.25 Effect of hole arrangement

No general conclusions may be drawn from the disposition of holes in a baffle. Various arrangements of holes, for a constant area ratio, lead to negligible changes in the overall loss factor.

3.26 Effect of hole inclination

To determine the effect of inclination of the plane of the hole to the air stream a series of cones were tested in which the cone angle was varied but the area ratio and hole arrangement remained the same. When the holes were placed normal to the airstream minimum loss was obtained. As the angle between the axes of the holes and the airstream (θ) increased the loss increased approximately as $\cos^2 \theta$ as shown in Figure 12. This is to be expected since the projected area of the holes on a plane normal to the air flow is directly proportional to $\cos \theta$ and loss is proportional to the square of the area ratio. Figure 13 shows relative loss defined as $\frac{\text{loss factor at inclination } \theta}{\text{loss factor at } \theta = 0 \text{ (i.e. minimum loss)}}$ plotted against θ. Placing the cone apex upstream or downstream had no measurable effect on the loss.

3.27 Effect of turbulence

Reference 14 gives details of experiments carried out on a series of flat plates which illustrate the effect of turbulence on drag. Figure 14 shows the variation of pressure drop coefficient (static pressure difference/free stream velocity head) with percentage turbulence. The percentage turbulence is defined as

$$\frac{\text{root mean square of speed fluctuation}}{\text{average speed}} \times 100$$

The turbulence level was varied by placing large wire diameter, large mesh gauzes upstream of the test section. Considering practical applications, the change of percentage turbulence is usually small in a given test set up, but this feature of drag increase with percentage turbulence is important when comparing pressure loss measurements made on an identical component on two dissimilar rigs. However, reference to Figure 14 shows that percentage turbulence changes will only account for small differences in pressure loss.

3.3 Gutter stabilisers

The loss due to gutters is mainly an expansion loss arising from the fuel injector situated in the high velocity throat and also the diffusion loss up to the chamber cross-section from the downstream end of the gutter. For incompressible flow the loss is $(\lambda - 1)^2$ and includes a discharge coefficient for the gutter. For included gutter angles up to 15° the value of C_d is about unity. For higher angles the C_d decreases fairly rapidly, probably following a cosine law, but this is merely a hypothesis which, although qualitatively correct, should be confirmed experimentally before being used indiscriminately. If the throat velocity is greater than 200 ft./sec. the curves of Reference 11 should be used to allow for compressibility in determining the pressure loss.

For hot running the fundamental pressure loss due to heat addition (see Section 6.0) is added to the cold loss. The result obtained may be high compared with the experimental value. This is due to the aerodynamic flow pattern around the gutter being significantly altered by combustion. The principal effects of combustion are to reduce the strength of the reverse flow (and hence the pressure loss) and to increase the length and breadth of the wake. A further contribution to the loss factor is the dissipation of the upstream component of the fuel momentum when injected in the throat. If the inlet air and fuel temperatures are substantially the same, increase in fuel flow results in an increase in pressure loss (of the order 3-5 per cent), but if the air temperature is high compared with the fuel the pressure loss tends to decrease. This later phenomenon is due to the reduction in air temperature due to fuel vaporisation. The presence of the fuel increases the effective blockage at the throat, and since the throat velocity and permanent blockage are both high, exerts a measurable effect on the loss. If the throat section is long friction effects must be taken into account by the modified "Fanning Equation"

$$\frac{d\,(\Delta P)}{d\ell} = 4\,\frac{f}{D} \cdot \frac{1}{2}\,\rho\, V^2 \qquad \ldots\ \ldots\ \ldots\ \ldots \qquad (34)$$

for rectangular or annular cross-sectional areas the equivalent diameter (d_e) is used. (f) will vary between 0.002 and 0.008 depending on the Reynolds number as shown in Figure 15.

The effect on pressure loss of using skirted gutters (see Figure 16, (a) and (b)) as opposed to the conventional type is negligible, although an improvement in flame stability may result. The use of "finger" type flame spreaders attached to the downstream end of the gutter gives rise to a small increase in the loss which is accounted for approximately by the loss due to flow through the projected free area of the fingers in the plane of the gutter base as shown in Figure 16(c). This loss will probably be a little higher than the more gradual loss occurring along the fingers, but does give

a basis for analytical determination. Diffusion losses can be treated by the method given in Section 7.1.

From the preceding paragraph it is obvious that the pressure loss picture is far from complete, but correlation of the results of many experiments now in progress will improve the position.

4.0 Cooling losses

The main types of cooling device in use at the present time are the louvre, porous wall and boundary layer systems. For a detailed analysis and description of these systems Reference 15 should be consulted. From the point of view of pressure loss no new problems are involved, each system merely utilising the available pressure difference between the primary and secondary flow paths.

4.1 Porous wall

This method of cooling is among the more efficient and is amenable to analytical treatment. The pressure drop for laminar flow through a porous material is given by D'Arcy's equation

$$\frac{Q.L.}{p_1^2 - p_2^2} = \frac{Z}{144} \cdot \frac{\rho 2}{2\, p_2\, \mu} \quad .. \quad .. \quad .. \quad .. \quad (35)$$

where p_1 and p_2 are the air pressures in lb./ft.^{2} on either side of the porous wall and Z is the coefficient of permeability and has dimensions of an area, usually square inches. For the small pressure differences available in combustion chambers

$$p_1^2 - p_2^2 \simeq 2\, p_2 \cdot \Delta p \text{ where } \Delta p = \text{pressure drop}$$

thus

$$\frac{Q.L.}{\Delta p} = \frac{Z}{144} \frac{\rho}{\mu} \quad .. \quad .. \quad .. \quad .. \quad (36)$$

However, Z must be determined experimentally in the first instance, and may decrease with operating time due to deposition in the pores. Typical values of Z are 10^{-8} to 10^{-10} in^2.

4.2 "Louvred" surface cooling

The "louvred" wall is essentially a mode of construction (British Patent No.642,257 held by "Shell" Refining and Marketing Company Limited) by which the effective area for heat transfer is considerably increased. The surface to be cooled is constructed so that there are many small independent passages along which the cooling air may flow radially, finally emerging to mix with the primary stream. To estimate the pressure drop associated with the flow of air through the passages in the "louvred wall" under turbulent flow conditions, Blazius' Equation is used:-

$$\Delta P = \frac{0.316}{Re^{0.25}} \cdot \frac{\rho V^2}{2} \frac{L}{d_e} \quad .. \quad .. \quad .. \quad .. \quad .. \quad .. \quad (37)$$

for laminar flow conditions:-

$$\Delta P = \frac{96}{Re} \frac{\rho V^2}{2} \cdot \frac{L}{d_e} \quad .. \quad .. \quad .. \quad .. \quad .. \quad .. \quad (38)$$

The criterion for turbulent or laminar flow is whether Re is above or below 2,000. In addition the injection loss = $\frac{1}{2} \rho V^2$ should be added to either Equation (37) or (38) to give the complete loss.

4.3 Combination of external air flow and localised air injection cooling

This method requires the cooling air to flow in an annular sheath in an upstream axial direction and then to inject it through small holes in the flame tube into the high temperature side where it forms a blanketing annular layer. The pressure drop is the sum of the friction drop given by Equations (37) or (38) and the injection loss which will be due to accelerating the air up to the required injection velocity. The latter loss is given by

$$\Delta P = \frac{1}{2} \rho \left(\frac{V_h}{0.61} \right)^2 \quad .. \quad .. \quad .. \quad .. \quad .. \quad .. \quad (39)$$

where V_h is the velocity based on total port area and 0.61 is the discharge coefficient.

The overall loss for this cooling system is

$$\Delta P = \frac{0.316}{Re^{0.25}} \frac{\rho V^2}{2} \cdot \frac{L}{d_e} + \frac{\rho}{2} \left(\frac{V_h}{0.61} \right)^2 \quad .. \quad .. \quad .. \quad .. \quad (40)$$

5.0 Mixing losses

Up to this Section most of the information is complete and valid for all types of combustion chamber but an incomplete knowledge of the mixing process restricts the application to low speed chambers.

The pressure loss due to mixing is probably the most difficult loss to determine analytically without some experimental assistance, since it affects both the primary and secondary streams. The part of the mixing loss attributable to the secondary circuit is almost entirely due to expansion through the mixing holes. The loss associated with the primary circuit is

made up of the flow through the effective blockage due to the radial "spokes" of cold air and the subsequent macro-turbulence.

5.1 Secondary mixing losses

As stated in the previous Section the secondary mixing loss is given approximately by the velocity head through the holes. This requires a knowledge of the discharge coefficient, which is subject to a wide variation depending on hole area, outer duct area and the percentage flow from the outer duct through the hole. Figure 17 is a curve of C_d versus a factor $\frac{F}{B}$ where F is the percentage flow from the outer duct and B is the ratio of hole area/outer duct area. This curve was taken from Reference 16 and is the result of water model tests with hole sizes ranging from 0.6 to 1.9 in. diameter. It is satisfactory to determine the percentage flow through the hole on an area basis.

Darling[17] has also studied this problem using air as the flow medium and presents his values of discharge coefficient as a function of the "Approach Velocity Factor", i.e. $\frac{V_1}{V_2}$ where V_1 is the mean velocity in the approach channel, and V_2 is the mean velocity through the hole. The number of experimental points taken are less than in Reference 17 and only one size of hole was used. Darling's results have been plotted on the same abscissa as the Lucas results in Figure 17. The curves are of similar shape although the curve for air is some 7 per cent higher. For equal conditions of flow the discharge coefficient for air would be higher due to compressibility although by a very small amount. The real difference appears to be due to the positioning of the static taps on the two separate rigs. For the water model they are situated in the annulus some $2\frac{3}{4}$ in. upstream of the injection hole axis whereas for the air tests the tap was situated on the outer annulus wall directly above the centre of the hole. The maximum value of C_d obtained in Reference 17 is higher than anticipated for this type of discharge. The true values for air are probably a little higher than the water results although negligible error will result in applying these directly to air calculations.*

The secondary pressure loss due to mixing will then be given by

$$\Delta P = \frac{1}{2} \rho \left(\frac{V_h}{C_d}\right)^2 \qquad .. \quad .. \quad .. \quad .. \quad (41)$$

C_d being obtained from Figure 17.

---

*This statement is confirmed by an American Report "Can Burner Hole Discharge Coefficient Investigation" Consolidated Vultee Aircraft Corporation No.6149, just received.

For holes inclined to the direction of flow the discharge coefficient obtained from Figure 17 should be increased by the root of the relative loss factor since $C_d \propto \frac{1}{\sqrt{\theta}}$. For example, if the mixer has a semi-angle of 15° then with reference to Figure 13, $\theta = 75°$, and C_d obtained from Figure 16 is multiplied by $\sqrt{\frac{1.482}{1.452}}$.

The preceding statements assume that the hot stream effects are negligible. This is probably true for low speed industrial type chambers but evidence from experiments now in progress suggests that the hot stream momentum substantially affects the result and reduces the value of the pressure drop as given by Equation (41).

5.2 Primary mixing losses

Losses in the hot stream from the injection plane to the "mixed" plane are approximately half the velocity head at the plane of injection and are thus very small. For very large or industrial type chambers it can be regarded as negligible. This part of the work will be in a much more exact form when the results of mixing experiments now in progress are available.

6.0 Heat addition losses

If, as is usual, the combustion occurs in a parallel duct immediately downstream of the primary baffle the "fundamental" loss of pressure is given by

$$\Delta P = \frac{1}{2} \rho_1 V_1^2 \left(\frac{\rho_1}{\rho_2} - 1 \right) \quad .. \quad .. \quad .. \quad .. \quad (42)$$

and if the static pressure difference is small

$$\Delta P = \frac{1}{2} \rho_1 V_1^2 \left(\frac{T_2}{T_1} - 1 \right) \quad .. \quad .. \quad .. \quad .. \quad (42a)$$

In the case of a varying cross-sectional area in the flame tube, it is best to consider in detail the relative proportions of heat release as in Section 2.3.

7.0 Miscellaneous losses

7.1 Diffusion losses

For various reasons the reduction of velocity in the compressor diffuser is often limited and the inlet velocity to the combustion chamber is frequently greater than 300 ft./sec., the exact value depending to a large extent on the type of compressor. Typical values for the velocity in the secondary annulus are of the order of 150 ft./sec. and it is necessary to reduce the inlet air velocity to that existing in the secondary annulus as efficiently as possible. The efficiency of a diffuser may be defined by a

factor (e) which gives the efficiency of conversion of velocity head to static pressure

$$\therefore \quad P_2 - P_1 = e \frac{\rho}{2g} (v_1^2 - v_2^2) \quad .. \quad .. \quad .. \quad (43)$$

$$\therefore \text{ total pressure loss } P_1 - P_2 = (1 - e) \frac{\rho}{2g} (v_1^2 - v_2^2) \quad .. \quad .. \quad (44)$$

$$\therefore \quad \text{loss factor } \Phi = (1 - e) \left\{ 1 - \left(\frac{A_1}{A_2} \right)^2 \right\} \quad .. \quad .. \quad (45)$$

Values of (e) have been taken from Reference 18 which agree with experimental results given in Reference 19 and are plotted in Figure 18 against total diffuser angle θ. A recent report[20] has shown that assymmetry of the inlet velocity distribution has a marked effect on diffuser efficiency especially for large diffuser angles. A low velocity region near the wall is equally undesirable.

7.2 Losses due to bends

Although not explicitly a component of the combustion chamber, bend entries and exits for combustion chambers are relatively common and their loss is frequently included in the overall chamber loss figure. Accurate data for the losses in bends is given in Reference 21, but in general terms it can be stated that, for a bend without diffusion and with a directional change not exceeding 90°, and having a mean radius not less than 1.5 times the duct diameter or passage width, the pressure loss will not exceed half the velocity head. The loss round a sharp bend can be reduced by imparting an acceleration to the air.

Cascade bends are now universally employed in gas turbine systems by virtue of their efficiency both in terms of pressure drop and their ability to turn the air through a desired angle. Reference 22 gives the design details and procedure for constructing a bend in which the blades are spaced in an arithmetic progression from the inside radius. The pressure loss associated with such a bend is affected by size and manufacturing variations (especially internal finish) but a loss figure of 25 per cent of the velocity head through the bend is sufficiently accurate for most purposes.

7.3 Losses due to corrugated spacers

This form of construction is now used frequently as a mechanical spacer for skin cooling of combustion chamber walls. The discharge coefficient of this spacer was investigated[23] on a water model and found to be 0.8 when based on the drawing dimensions and 0.9 in terms of the actual measured areas. The variation in drawing and measured dimensions is due to manufacturing difficulties principally in the welding operation. For design purposes the estimated area of the section is used for which C_d equals 0.8.

7.4 Friction losses

In the majority of chambers the friction losses are usually negligible compared with the individual component losses but in a few isolated cases there are long sections where frictional affects are measurable.

The pressure drop is given by the modified "Fanning Equation"

$$\frac{d(\Delta P)}{d\ell} = 4\frac{f}{D} \cdot \frac{1}{2}\rho V^2 \qquad .. \quad .. \quad .. \quad (34)$$

f being obtained from Figure 15.

For irregular shaped ducts and annuli the hydraulic mean diameter d_e is used for D.

i.e. $D = 4\frac{A}{S}$

8.0 Overall chamber loss

Having considered in some detail the pressure losses caused by the various components of the chamber, it is now necessary to see how they may be linked to give a value of the loss coefficient for a particular flow path. For consecutive losses in a flow path the overall loss coefficient is merely the arithmetic sum of the individual loss factors provided they are expressed in terms of the same reference velocity head. For losses occurring in parallel circuits the method of Probert and Kielland[1] is used. A loss coefficient is applied to each flow path such that the total head loss in the stream is equal to the loss coefficient times the velocity head at some reference area. On the further assumption that the static pressures are equal in both streams at divergence and confluence an expression for the overall loss factor is obtained. While this method proves satisfactory for the simpler types of chamber a considerable amount of calculation is required if there are more than two general flow paths. Also, because of the "step-by-step" method of calculation, if the loss factor of one of the components is changed a complete recalculation is necessary.

Reference 2 is based on the same principles and assumptions as stated above but as shown in Appendix II reduces the complexity and quantity of calculation.

If ϕx = pressure loss factor of a circuit in terms of velocity head at area x

and ϕy = same loss in terms of velocity head at area y

then $$\frac{\phi x}{\phi y} = \left(\frac{x}{y}\right)^2 \qquad .. \quad .. \quad .. \quad .. \quad .. \quad .. \quad (46)$$

and in the event of a density change

$$\frac{\phi x}{\phi y} = \left(\frac{x}{y}\right)^2 \left(\frac{\rho y}{\rho x}\right) \qquad .. \quad .. \quad .. \quad .. \quad .. \quad .. \quad (47)$$

Thus by applying this relation it is possible to express all individual loss factors in terms of the velocity heads, due to each flow, at the same cross-sectional area. This reference area is purely arbitrary and can be the chamber entry area, flame tube area or casing area.

Since the total head drop of any flow circuit in the chamber must be the same

$$\phi_1 \, q_1 = \phi_2 \, q_2 = \phi_3 \, q_3 = \Phi . q. \qquad .. \quad .. \quad .. \quad .. \quad (48)$$

where q_1, q_2 ..... etc. are the velocity heads due to the individual flows in the reference area, and ϕ_1, ϕ_2 ..... etc. are the loss factors expressed in terms of the velocity head at the reference area by means of Equation (47).

But $q \propto W^2$ since ρ is assumed constant at the reference area for all flows

$$\therefore \qquad W_1 \sqrt{\phi_1} = W_2 \sqrt{\phi_2} = W_3 \sqrt{\phi_3} \text{ etc.} \qquad .. \quad .. \quad .. \quad .. \quad (49)$$

and the overall loss factor by

$$\Phi = \phi_1 \left(\frac{W_1}{W}\right)^2 = \phi_2 \left(\frac{W_2}{W}\right)^2 \text{ etc.} \qquad .. \quad .. \quad .. \quad .. \quad (50)$$

also since the sum of the percentage flows through each circuit must equal the total flow

$$W = 100 = W_1 + W_2 + W_3 \text{ etc.} \qquad .. \quad .. \quad .. \quad .. \quad (51)$$

thus any required circuit flow say W_1 is given by:

$$W_1 = 100 - W_2 - W_3$$

$$= 100 - W_1 \left(\frac{\phi_1}{\phi_2}\right)^{\frac{1}{2}} - W_1 \left(\frac{\phi_1}{\phi_3}\right)^{\frac{1}{2}}$$

$$W_1 = \frac{100}{1 + \left(\frac{\phi_1}{\phi_2}\right)^{\frac{1}{2}} + \left(\frac{\phi_1}{\phi_3}\right)^{\frac{1}{2}}} \qquad .. \quad .. \quad .. \quad .. \quad (52)$$

assuming there is a total of three circuits.

9.0 Conclusions

By means of the analysis of component pressure losses in this Report it should be possible to make a reasonably accurate theoretical calculation of the cold air flow distribution and overall loss factor of a combustion chamber. Certain limitations in our knowledge of compressible flow characteristics especially mixing of gas streams, imposes a restriction on the accuracy for high velocity chambers. This contingency will be obviated by experimental work now in hand. The comparison between calculated and measured pressure drop for a typical combustion chamber as shown in Appendix II is good. The percentage difference may be fortuitous but the prospects of calculating the cold pressure drop of a chamber from the design drawing with an accuracy of ± 5 per cent seems favourable. Assuming the mixing experiments improve the 'hot' pressure loss calculations, the method can probably be further refined by comparing calculated and measured results from a variety of chambers.

REFERENCES

No.	Author(s)	Title
1	R. P. Probert and A. Kielland	Experiments on Combustion Chamber Pressure Loss. Power Jets Report No. R.1164. December 1945.
2	R. B. Walker	Unpublished Work at N.G.T.E.
3	H. A. Knight	Unpublished Work at N.G.T.E.
4	Durand	Aerodynamic Theory. Vol. 2, pp.91-96. (Reprinted) January 1943.
5	I. Berenblut	The Pressure Losses in Combustion Chambers with Swirl Air Directors. Shell Report ICT/20. December 1948.
6	D. G. Ainley and G. C. R. Mathieson	An Examination of the Flow and Pressure Losses in Blade Rows of Axial Flow Turbines. N.G.T.E. Report No. R.86. March 1951.
7	D. G. Ainley and G. C. R. Mathieson	A Method of Performance Estimation for Axial Flow Turbines. N.G.T.E. Report No. R.111. December 1951.
8	D. G. Ainley	Proceedings Institution of Mechanical Engineers, 1948, Vol.159 (W.E.I. No.41).
9	R. P. Probert and H. A. Knight	Unpublished Work at N.G.T.E.
10	H. A. Knight	Baffle Pressure Loss Experiments. N.G.T.E. Memorandum No. M.161 (to be published).
11	H. A. Knight	Theoretical Investigations into Baffle Pressure Losses. N.G.T.E. Memorandum No. M.52. June 1949.
12	E. E. Callaghan and D. T. Bowden	Investigation of Flow Coefficient of Circular, Square and Elliptical Orifices at High Pressure Ratios. N.A.C.A. Tech. Note No.1947. September 1949.
13	-	B.S. Code 1042. Flow Measurement. 1943.
14	G. B. Schubauer and H. L. Dryden	The Effect of Turbulence on the Drag of Flat Plates. N.A.C.A. Report No.546. 1935.
15	F. J. Bayley	Air Cooling Methods for Gas Turbine Combustion Systems. N.G.T.E. Report No. R.101. August 1951.

REFERENCES (Cont'd.)

No.	Author(s)	Title
16	D. J. Miller	The Coefficient of Discharge of a Circular Hole in the Wall of a Duct. Lucas Report B.41,349. January 1951.
17	R. F. Darling	Tests on the Flow of Dilution Air through a Hole in a Flame Tube. Pametrada Report No.52. November 1949.
18	N. A. Hall	Thermodynamics of Fluid Flow. Wiley 1951.
19	A. H. Gibson	Hydraulics and its Applications. Constable & Company Limited, 4th Edition. 1946.
20	I. H. Johnson	The Effect of Inlet Conditions on the Flow in Annular Diffusers. N.G.T.E. Memorandum No. M.167. January 1953.
21	S. Gray	A Survey of Existing Information on the Flow in Bent Channels and the Losses Involved. Power Jets Report No.R.1104. June 1945.
22	N. A. Dimmock	The Development of a Simply Constructed Cascade Corner for Circular Cross-Section Ducts. N.G.T.E. Memorandum No. M.78. February 1950.
23	D. J. Miller	The Coefficient of Discharge of a Gap Containing a Corrugated Spacer. Lucas Report B.41,689. March 1952.

ADVANCE CIRCULATION BY N.G.T.E.

CS(A)
The Chief Scientist
CGWL
DGTD(A)
PDSR(A)
PDERD
DERD
NA/DERD
DIGT
AD/Eng.R
AD/Eng.RD1
AD/Eng.RD2
AD/Eng.RD6
Pats.1(c)
TPA3/TIB(M)Dist. - 257 copies

HAK/RBW/BBMP/292/44/19/3.12.53

APPENDIX I

Symbols

A	=	Cross-sectional area	- ft.^{2}
B	=	Ratio $\frac{\text{hole area}}{\text{outer duct area}}$ (see Figure 17)	dimensionless
C	=	Constant for vortex decay law	
c	=	Blade chord	
C_d	=	Discharge coefficient	dimensionless
C_L	=	Lift coefficient (see Equations 9 and 10)	dimensionless
D	=	Outer diameter	- ft.
d	=	Inner diameter	- ft.
d_e	=	Equivalent diameter = $4 \times \frac{\text{cross-sectional area}}{\text{perimeter}}$	- ft.
e	=	Diffuser efficiency	dimensionless
F	=	Percentage flow from outer duct (see Figure 17)	dimensionless
f	=	Friction factor (see Equation 34)	dimensionless
G	=	Heat release factor (see Equation 31)	dimensionless
H	=	Total energy per unit mass	- ft.^{2} sec.$^{-2}$
K	=	Secondary loss factor (see Equation 10)	dimensionless
L, ℓ	=	Length	- ft.
M	=	Mach number	dimensionless
M_v	=	Mach number at vena-contracta	dimensionless
m	=	Area ratio = $\frac{d^2}{D^2}$	dimensionless
n	=	Index in vortex decay law	dimensionless
P	=	Total pressure	- lb. ft.$^{-2}$
p	=	Static pressure	- lb. ft.$^{-2}$
ΔP	=	Total pressure loss	- lb. ft.$^{-2}$
Δp	=	Static pressure loss	- lb. ft.$^{-2}$
Q	=	Mass flow per unit cooled surface area	- slugs. sec.$^{-1}$ ft.$^{-2}$
R, r	=	Radii	- ft.

APPENDIX I (Cont'd.)

Re	=	Reynolds number	dimensionless
S	=	Perimeter	- ft.
s	=	Pitch	- ft.
t	=	Blade thickness	- ft.
V	=	Absolute velocity	- ft. sec.$^{-1}$
V_h	=	Velocity through hole	- ft. sec.$^{-1}$
V_w	=	Whirl velocity	- ft. sec.$^{-1}$
W	=	Weight flow	- lb. sec.$^{-1}$
x	=	Area	- ft.^{2}
Y_p	=	Profile loss coefficient	dimensionless
Y_s	=	Secondary loss coefficient	dimensionless
Y_t	=	Total loss coefficient	dimensionless
y	=	Area	- ft.^{2}
Z	=	Coefficient of permeability (see Equation 36)	- in.^{2}
α	=	Outlet air angle	dimensionless
β	=	Blade outlet angle	dimensionless
γ	=	Ratio of specific heats	dimensionless
θ	=	Baffle semi-cone angle	dimensionless
λ	=	Effective area ratio	dimensionless
μ	=	Viscosity	- slugs. ft.$^{-1}$ sec.$^{-1}$
ρ	=	Density	- slugs.ft.$^{-3}$
ρ'	=	Flame tube density (see Figure 9)	- slugs.ft.$^{-3}$
ρ''	=	Throat density (see Figure 9)	- slugs.ft.$^{-3}$
σ	=	Pitch chord ratio = $\frac{s}{c}$	dimensionless
ϕ, ϕ	=	Loss coefficient = $\frac{P_1 - P_2}{\frac{1}{2} \rho_1 V_1^2}$	dimensionless
ω	=	Swirl angle for vortex swirler (see Section 2.26)	dimensionless

APPENDIX I (Cont'd.)

Suffices

$( )_o$ = Known condition usually inner radius

$( )_1$ = Entry or initial condition

$( )_2$ = Outlet or final condition

$( )_F$ = Pertaining to flame tube

$( )_m$ = Pertaining to mean radius

$( )_s$ = Pertaining to swirler or secondary

$( )_t$ = Throat condition

APPENDIX II

Air flow distribution and overall loss factor for a conventional chamber (Rolls Royce R.M.60 Model)

As can be seen from Figure 19 the air flow is divided into eight separate flow circuits. Each individual loss factor will be expressed in terms of the velocity head pertaining to the overall chamber cross-sectional area.

To determine the "hot" distribution case at a given temperature ratio the cold distribution is used to calculate the primary combustion zone temperature. Strictly, a method of successive approximation should be used to allow for small redistributions of air flow but the magnitude of the errors involved and the general accuracy of the method as a whole do not warrant it.

Calculation of individual loss factors

(1) Expansion ratio through primary orifice

$$= \frac{2.91}{0.84} = 3.47 \quad \text{i.e. } m = 0.312$$

From Figure 11

$$C_d = 0.6 \times 1.058 = 0.635$$

The effect of the shoulder will certainly reduce the discharge and a C_d of 0.6 is used.

$$\text{Loss through orifice} = (\lambda - 1)^2 = \left(\frac{3.47}{0.6} - 1\right)^2 = \underline{22.8}$$

$$\text{In terms of reference } \phi = 22.8 \times \left(\frac{38.5}{2.91}\right)^2 = \underline{3,990}$$

Considering the swirler

$$\alpha = 54^\circ \qquad A_F = 21.3 \text{ in.}^2 \qquad A_S = 2.6 \text{ in.}^2$$

By Equation (12)

$$\Phi_F = 1.15\left(\frac{21.3}{2.6}\right)^2 \frac{1}{(0.5878)^2} - 1$$

$$= \underline{222}$$

APPENDIX II (Cont'd.)

In terms of reference area $\phi = 222 \times \left(\frac{38.5}{21.3}\right)^2$

$= 725$

The overall loss for the two resistances in series is the algebraic sum of the loss factors (when expressed in terms of the same area).

$\therefore$ Loss through No.1 Circuit = $\phi_1 = 4,715$

(2) Loss through corrugated spacer

Free area = 1.07 in.^{2}

Expanded area = 2.43 in.^{2}

from Section 7.30 $C_d = 0.8$

Loss in terms of reference area = $\left(\frac{2.43}{1.07 \times 0.8} - 1\right)^2 \left(\frac{38.5}{2.43}\right)^2 = 850$

'Expansion' loss after spacer in terms of reference are

$= \left\{\left(\frac{21.3}{2.43}\right) - 1\right\}^2 \left(\frac{38.5}{21.3}\right)^2 = 197$

Loss through No.2 Circuit = $\phi_2 = 1,047$

(3) Loss through primary holes

Firstly, the C_d of the holes must be estimated by the method outlined in Section 5.10 and Figure 17.

F is determined on an area basis only

$$F = \frac{100 \times 1.39}{1.39 + 0.48 + 0.55 + 3.49 + 1.99 + 3.49}$$

$$= \frac{139}{11.39} = 12.2 \text{ per cent}$$

APPENDIX II (Cont'd.)

$$B = \frac{1.39}{16.6} = 0.0837$$

$$\frac{F}{B} = \frac{12.2}{0.0837} = 146$$

From Figure 17 $C_d = 0.582$

$$\text{Loss in terms of reference area} = \left(\frac{21.3}{1.39 \times 0.582} - 1\right)^2 \left(\frac{38.5}{21.3}\right)^2$$

$$\underline{\underline{\phi_3 = 2,090}}$$

(4) Loss through first row of cooling holes

$$F = \frac{100 \times 0.48}{10.0} = 4.80 \text{ per cent}$$

$$B = \frac{0.48}{16.6} = 0.0289$$

$$\frac{F}{B} = \frac{4.80}{0.0289} = 166$$

From Figure 17 $C_d = 0.595$

Since these holes are inclined at an angle of 17° the discharge coefficient is increased (see Section 5.10 and Figure 13).

$$C_d = 0.595 \times \sqrt{\frac{1.482}{1.442}} = 0.603$$

It is assumed that the air entering these holes forms an annular sheath which does not substantially increase in thickness as it flows downstream.

$$\text{loss factor } \phi_4 = \left(\frac{23.8 - 21.3}{0.603 \times 0.48} - 1\right)^2 \left(\frac{38.5}{2.5}\right)^2 = 13,800$$

$$\underline{\underline{\phi_4 = 13,800}}$$

APPENDIX II (Cont'd.)

(5) Loss through second set of cooling holes

$$F = \frac{100 \times 0.55}{9.52} = 5.78 \text{ per cent}$$

$$B = \frac{0.55}{14.1} = 0.039$$

$$\frac{F}{B} = \frac{5.78}{0.039} = 148$$

From Figure 17 C_d = 0.585

Since holes are inclined at 20°, from Figure 13 C_d is increased

$$C_d = 0.585 \times \sqrt{\frac{1.482}{1.426}} = 0.596$$

assuming the air forms an annular sheath as before

$$\phi_5 = \left(\frac{26.6 - 23.8}{0.596 \times 0.55} - 1\right)^2 \left(\frac{38.5}{2.8}\right)^2 = 10,700$$

$$\underline{\underline{\phi_5 = 10,700}}$$

(6) Loss through first row of mixing holes

$$F = \frac{100 \times 3.49}{8.975} = 38.9 \text{ per cent}$$

$$B = \frac{3.49}{11.3} = 0.309$$

$$\frac{F}{B} = \frac{38.9}{0.309} = 126$$

∴ From Figure 17 C_d = 0.564

APPENDIX II (Cont'd.)

$$\text{Mixing loss} = \frac{1}{2}\rho\left(\frac{V_h}{C_d}\right)^2$$

$$\therefore \quad \phi_6 = \left(\frac{1}{0.564}\right)^2\left(\frac{38.5}{3.49}\right)^2 = 383$$

$$\underline{\underline{\phi_6 = 383}}$$

(7) Loss through third set of cooling holes

$$F = \frac{100 \times 1.99}{1.99 + 3.49} = \frac{199}{5.48} = 36.3 \text{ per cent}$$

$$B = \frac{1.99}{11.3} = 0.176$$

$$\therefore \quad \frac{F}{B} = \frac{36.3}{0.176} = 206$$

$$\therefore \quad C_d = 0.608$$

Since inclination is 20° C_d is further increased. From Figure 13

$$\therefore \quad C_d = 0.608 \times \sqrt{\frac{1.482}{1.426}} = 0.62$$

By Equation (41) the loss factor in terms of the hole

$$\text{area} = \left(\frac{1}{0.62}\right)^2 = 2.6$$

$$\therefore \quad \phi_7 = 2.6\left(\frac{38.5}{1.99}\right)^2 = 974$$

$$\underline{\underline{\phi_7 = 974}}$$

APPENDIX II (Cont'd.)

Equation (41) was used as it is very difficult to decide to which effective area the injected air eventually "expands".

(8) Loss through final mixing holes

$$F = 100 \text{ per cent}$$

$$B = \frac{3.49}{8.3} = 0.42$$

$$\frac{F}{B} = \frac{100}{0.42} = 238$$

$$\therefore \quad C_d = 0.61$$

$$\therefore \quad \phi_8 = \left(\frac{1}{0.61}\right)^2 \left(\frac{38.5}{3.49}\right)^2 = 327$$

$$\therefore \quad \underline{\phi_8 = 327}$$

Cold air distribution

$\phi_1 = 4,715$	$\sqrt{\phi_1} = 68.7$
$\phi_2 = 1,047$	$\sqrt{\phi_2} = 32.4$
$\phi_3 = 2,090$	$\sqrt{\phi_3} = 45.7$
$\phi_4 = 13,800$	$\sqrt{\phi_4} = 117.6$
$\phi_5 = 10,700$	$\sqrt{\phi_5} = 107.0$
$\phi_6 = 383$	$\sqrt{\phi_6} = 19.6$
$\phi_7 = 974$	$\sqrt{\phi_7} = 31.2$
$\phi_8 = 327$	$\sqrt{\phi_8} = 18.1$

APPENDIX II (Cont'd.)

By Equation (51)

$$W_1 = \frac{100}{1 + \frac{68.7}{32.4} + \frac{68.7}{45.7} + \frac{68.7}{117.6} + \frac{68.7}{107.0} + \frac{68.7}{19.6} + \frac{68.7}{31.2} + \frac{68.7}{18.1}}$$

$$= \frac{100}{1 + 2.12 + 1.50 + 0.58 + 0.64 + 3.51 + 2.20 + 3.80} = \frac{100}{15.35}$$

W_1 = 6.5 per cent

$$W_2 = \frac{100}{\frac{32.4}{68.7} + 1 + \frac{32.4}{45.7} + \frac{32.4}{117.6} + \frac{32.4}{107.0} + \frac{32.4}{19.6} + \frac{32.4}{31.2} + \frac{32.4}{18.1}}$$

$$= \frac{100}{0.47 + 1 + 0.71 + 0.27 + 0.30 + 1.65 + 1.04 + 1.79} = \frac{100}{7.23}$$

W_2 = 13.8 per cent

$$W_3 = \frac{100}{\frac{45.7}{68.7} + \frac{45.7}{32.4} + 1 + \frac{45.7}{117.6} + \frac{45.7}{107.0} + \frac{45.7}{19.6} + \frac{45.7}{31.2} + \frac{45.7}{18.1}}$$

$$= \frac{100}{0.66 + 1.42 + 1 + 0.39 + 0.43 + 2.34 + 1.47 + 2.53} = \frac{100}{10.24}$$

W_3 = 9.8 per cent

$$W_4 = \frac{100}{\frac{117.6}{68.7} + \frac{117.6}{32.4} + \frac{117.6}{45.7} + 1 + \frac{117.6}{107} + \frac{117.6}{19.6} + \frac{117.6}{31.2} + \frac{117.6}{18.1}}$$

$$= \frac{100}{1.71 + 3.63 + 2.57 + 1 + 1.10 + 6.00 + 3.77 + 6.50} = \frac{100}{26.28}$$

W_4 = 3.8 per cent

APPENDIX II (Cont'd.)

$$W_5 = \frac{100}{\frac{107}{68.7} + \frac{107}{32.4} + \frac{107}{45.7} + \frac{107}{117.6} + 1 + \frac{107}{19.6} + \frac{107}{31.2} + \frac{107}{18.1}}$$

$$= \frac{100}{1.56 + 3.30 + 2.34 + 0.91 + 1 + 5.42 + 3.43 + 5.90} = \frac{100}{23.86}$$

W_5 = 4.2 per cent

$$W_6 = \frac{100}{\frac{19.6}{68.7} + \frac{19.6}{32.4} + \frac{19.6}{45.7} + \frac{19.6}{117.6} + \frac{19.6}{107} + 1 + \frac{19.6}{31.2} + \frac{19.6}{18.1}}$$

$$= \frac{100}{0.28 + 0.60 + 0.43 + 0.17 + 0.18 + 1 + 0.63 + 1.08} = \frac{100}{4.37}$$

W_6 = 22.8 per cent

$$W_7 = \frac{100}{\frac{31.2}{68.7} + \frac{31.2}{32.4} + \frac{31.2}{45.7} + \frac{31.2}{117.6} + \frac{31.2}{107.0} + \frac{31.2}{19.6} + 1 + \frac{31.2}{18.1}}$$

$$= \frac{100}{0.45 + 0.96 + 0.68 + 0.26 + 0.29 + 1.59 + 1 + 1.72} = \frac{100}{6.95}$$

W_7 = 14.4 per cent

$$W_8 = \frac{100}{\frac{18.1}{68.7} + \frac{18.1}{32.4} + \frac{18.1}{45.7} + \frac{18.1}{117.6} + \frac{18.1}{107.0} + \frac{18.1}{19.6} + \frac{18.1}{31.2} + 1}$$

$$= \frac{100}{0.26 + 0.56 + 0.40 + 0.15 + 0.17 + 0.92 + 0.58 + 1} = \frac{100}{4.04}$$

W_8 = 24.7 per cent

Check:- 6.5 + 13.8 + 9.8 + 3.8 + 4.2 + 22.8 + 14.4 + 24.7 = 100 per cent

APPENDIX II (Cont'd.)

Overall cold loss factor by Equation (50)

$$\Phi = \phi_1 \left(\frac{W_1}{W}\right)^2 = 4,715 \left(\frac{6.5}{100}\right)^2 = \underline{19.9}$$

$$= \underline{19.9 \text{ in terms of reference velocity heads}}$$

Check:- $$\Phi = \phi_2 \left(\frac{W_2}{W}\right)^2 = 1,047 \left(\frac{13.8}{100}\right)^2 = 19.9$$

The measured value of the cold pressure loss factor was 20.7 an error of about 4 per cent.

Hot pressure loss

To determine the effect of heat addition it is necessary to arrive at a value for the primary temperature.

Using the previously determined air flow distribution and assuming circuits 1, 2 and 3 constitute the primary air flow.

Percentage primary air = 6.5 + 13.8 + 9.8 = 30.1 per cent

Neglecting specific heat variation and assuming:-

Inlet temperature = 200°C.

Outlet temperature = 700°C.

If T_1 is the primary absolute temperature

then $30.1\ T_1 + 69.9.473 = 100.973$

$$\therefore \quad T_1 = \frac{97,300 - 33,000}{30.1} = \frac{64,300}{30.1}$$

$$= 2,130°K.$$

By Equation (42a)

$$\text{Heat addition loss factor} = \left(\frac{2,130}{473} - 1\right)$$

APPENDIX II (Cont'd.)

and in terms of reference area

$$= \left(\frac{1,657}{473}\right)\left(\frac{38.5}{21.3}\right)^2 = 11.4$$

Overall primary loss factor excluding combustion loss is by Equation (50)

$$\phi_p = \Phi\left(\frac{W}{W_1 + W_2 + W_3}\right)^2 = 19.9 \times \left(\frac{100}{30.1}\right)^2 = \frac{19.9}{0.301^2} = 220$$

New primary loss factor including combustion loss will be 220 + 11.4 = 231.4.

Assuming the secondary loss factor remains constant

$$\phi_s = \frac{19.9}{(0.699)^2} = 40.8$$

∴ the new distribution is

$$Q_p \sqrt{231.4} = Q_s \sqrt{40.8}$$

∴ percentage through primary

$$= \frac{100}{1 + \sqrt{\frac{231.4}{40.8}}} = 29.5 \text{ per cent}$$

Thus heat addition has reduced the primary total flow by 30.1 - 29.5 = 0.6 per cent.

The new hot loss factor = 231.4 $(0.295)^2$ = 20.2

The measured hot loss factor for the assumed temperature rise was 25, an error of about 20 per cent.

APPENDIX III

Derivation of theoretical whirl and axial velocity distributions

The equation for radial equilibrium in vortex flow is

$$\frac{1}{\rho}\frac{dp}{dr} = \frac{V_w^2}{r} \qquad .. \quad .. \quad .. \quad .. \quad (1)$$

The total energy unit/mass at any radius r is given by Bernoulli's equation for a compressible fluid

$$H = \frac{V_a^2}{2} + \frac{V_w^2}{2} + \frac{\gamma}{\gamma - 1}\frac{p}{\rho} \qquad .. \quad (2)$$

Assuming the expansion to be

$$\frac{p}{\rho\gamma} = \text{constant} \qquad .. \quad .. \quad .. \quad .. \quad (3)$$

and that H is constant, we have by differentiating (2) and (3) that

$$V_a \frac{dV_a}{d_r} + V_w \frac{dV_w}{d_r} + \frac{1}{\rho}\frac{d_p}{d_r} = 0$$

and using (1)

$$V_a \frac{dV_a}{d_r} + V_w \frac{dV_w}{d_r} + \frac{V_w^2}{r} = 0 \qquad .. \quad .. \quad .. \quad .. \quad (4)$$

the general vortex law is

$$V_w r^n = C \qquad .. \quad .. \quad .. \quad .. \quad (5)$$

and also

$$\tan\alpha = \frac{V_w}{V_a} \qquad .. \quad .. \quad .. \quad .. \quad (6)$$

by (5) and (6)

$$V_a \tan\alpha\, r^n = C \qquad .. \quad .. \quad .. \quad .. \quad (7)$$

APPENDIX III (Cont'd.)

By differentiation

$$\tan\alpha\, r^n \frac{dV_a}{dr} + V_a \cdot \tan\alpha\, n\, r^{n-1} + V_a \cdot r^n \sec^2\alpha \frac{d\alpha}{dr} = 0$$

whence $$\frac{d\alpha}{dr} = -\frac{1}{2} \sin 2\alpha \left(\frac{1}{V_a}\frac{dV_a}{dr} + \frac{n}{r}\right) \quad .. \quad .. \quad .. \quad .. \quad (8)$$

differentiating (6)

$$\frac{dV_w}{dr} = \frac{dV_a}{dr} \tan\alpha + V_a \sec^2\alpha \frac{d\alpha}{dr}$$

$$\therefore \quad V_w \frac{dV_w}{dr} = V_a \frac{dV_a}{dr} \tan^2\alpha + V_a^2 \sec^2\alpha \tan\frac{d\alpha}{dr} \quad .. \quad .. \quad (9)$$

Substituting for $\frac{d\alpha}{dr}$ in (9) and then substituting for $V_w \frac{dV_w}{dr}$ and $\frac{V_w^2}{r}$ in (4) finally gives

$$V_a \frac{dV_a}{dr} + (1 - n)\, C^2\, r^{-(2n+1)} = 0$$

Integrating, using subscript 'o' to refer to conditions at the inner radius for convenience

$$V_a^2 = V_{a_o}^2 + C^2 \frac{(1-n)}{n}\left[\frac{1}{r^{2n}} - \frac{1}{r_o^{2n}}\right] \quad .. \quad .. \quad (10)$$

Free vortex blading

For free vortex flow $n = 1$

$\therefore$ from Equation (10) $V_a = V_{a_o} = \text{constant}$

APPENDIX III (Cont'd.)

and by Equation (7)

$$\tan \alpha = \frac{J}{r} \quad \text{where} \quad J = \text{constant} = \frac{C}{V_{a_o}}$$

now $$\sec^2 \alpha_m = 1 + \frac{C^2}{r_m^2 V_a^2}$$

now the weighted mean radius = $$r_m = \sqrt{\tfrac{1}{2}} \left(R^2 + r_o^2\right)^{\frac{1}{2}}$$

$$\therefore \quad \sec^2 \alpha_m = 1 + \frac{2 r_o^2 \tan^2 \alpha_o}{R^2 + r_o^2} \qquad .. \quad .. \quad .. \quad .. \quad .. \quad (11)$$

Forced vortex blading

For forced vortex flow $n = -1$

$\therefore$ from Equation (10) $$V_a^2 = V_{a_o}^2 - 2C^2 (r^2 - r_o^2)$$

and $$\tan \alpha = \frac{C_r}{\sqrt{V_{a_o}^2 - 2C^2 (r^2 - r_o^2)}}$$

$\therefore$ $$\tan \alpha_m = \frac{r_m}{\sqrt{\dfrac{r_o^2}{\tan^2 \alpha_o} - 2 (r_m^2 - r_o^2)}}$$

$$\sec^2 \alpha_m = 1 + \left[\frac{(R^2 + r_o^2)}{2\left\{\dfrac{r_o^2}{\tan^2 \alpha_o} - (R^2 - r_o^2)\right\}}\right]$$

$$= 1 + \frac{(R^2 + r_o^2) \tan^2 \alpha_o}{2\left\{r_o^2 \sec^2 \alpha_o - R^2 \tan^2 \alpha_o\right\}}$$

$$= 1 + \left\{\frac{(R^2 + r_o^2)}{2 (r_o^2 \operatorname{cosec}^2 \alpha_o - R^2)}\right\}$$

.. .. (12)

FIG. 1.

SK 57571

VARIATION OF AIR OUTLET ANGLE FOR FLAT PLATE CASCADES.

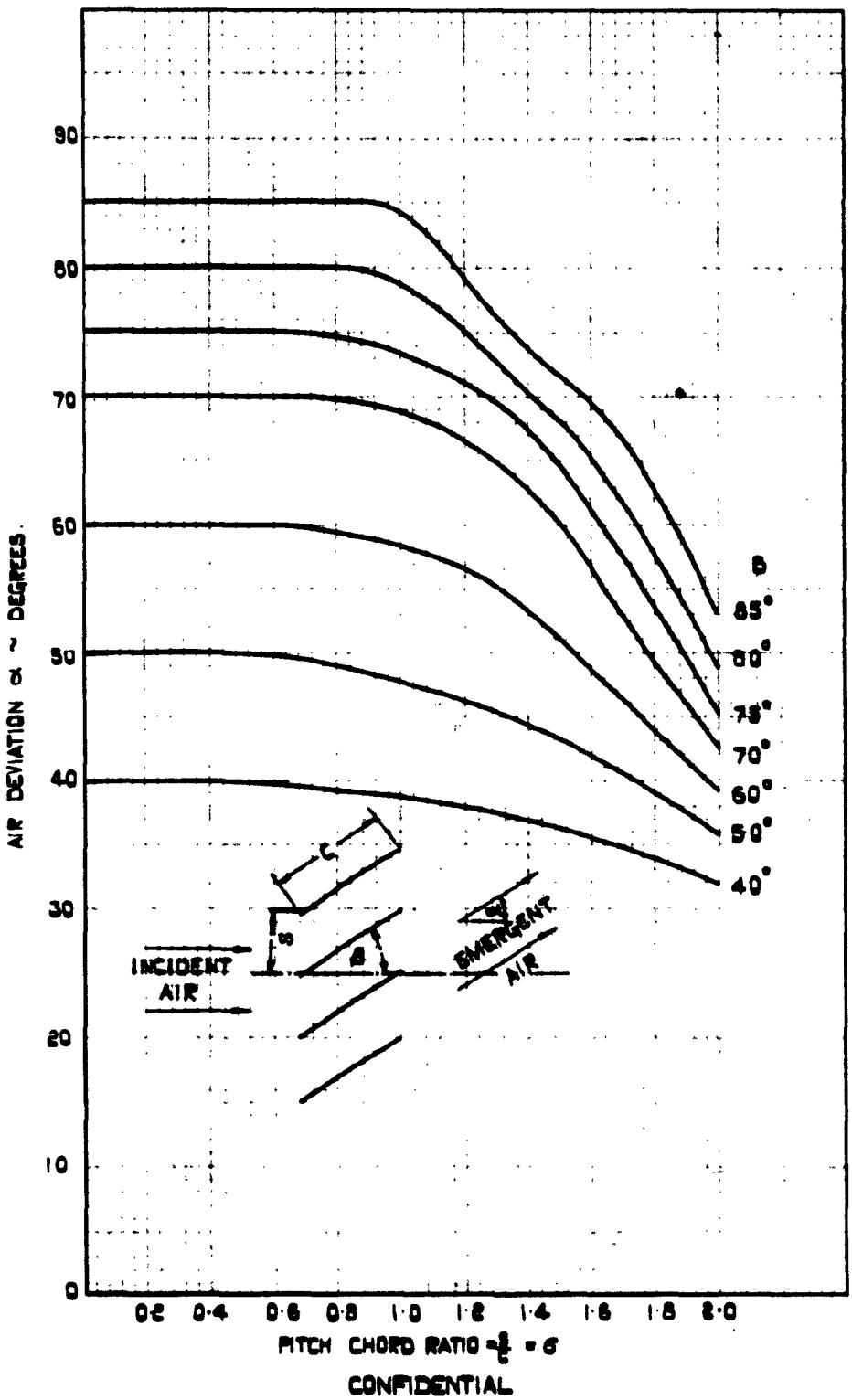

FIG. 2.

SWIRLER BLADE NOMENCLATURE

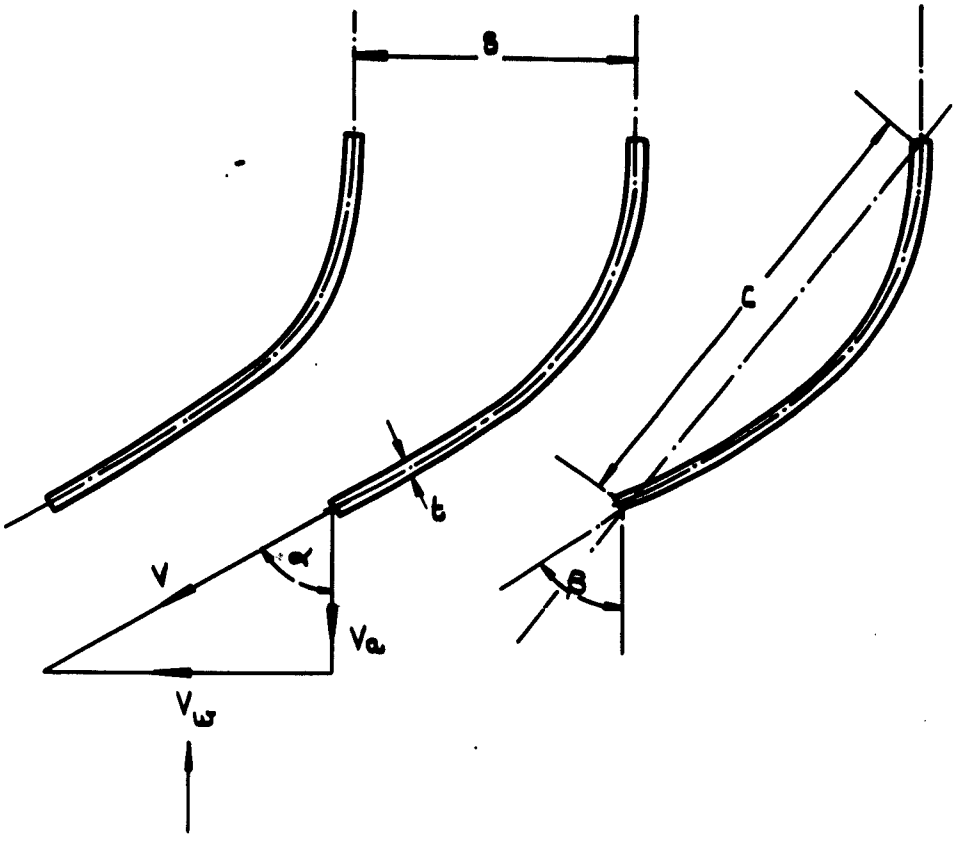

GAS OUTLET ANGLE NOTATION.

FIG. 3.

PROFILE LOSS COEFFICIENTS FOR ZERO INCIDENCE.

($t/c = 20\%$ $Re = 2 \times 10^5$ $M < 0.6$)

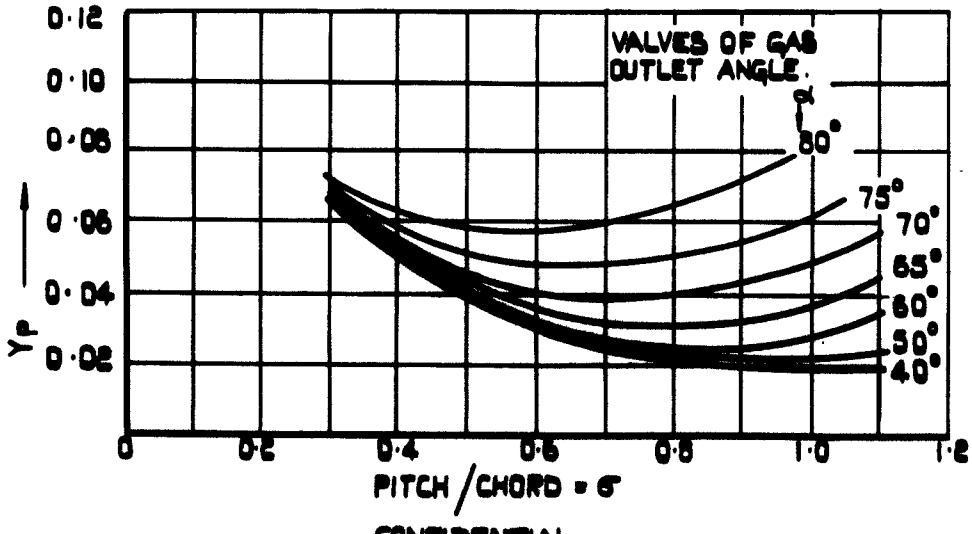

CONFIDENTIAL.

FIG. 4

SK57573

SECONDARY LOSSES IN BLADES.

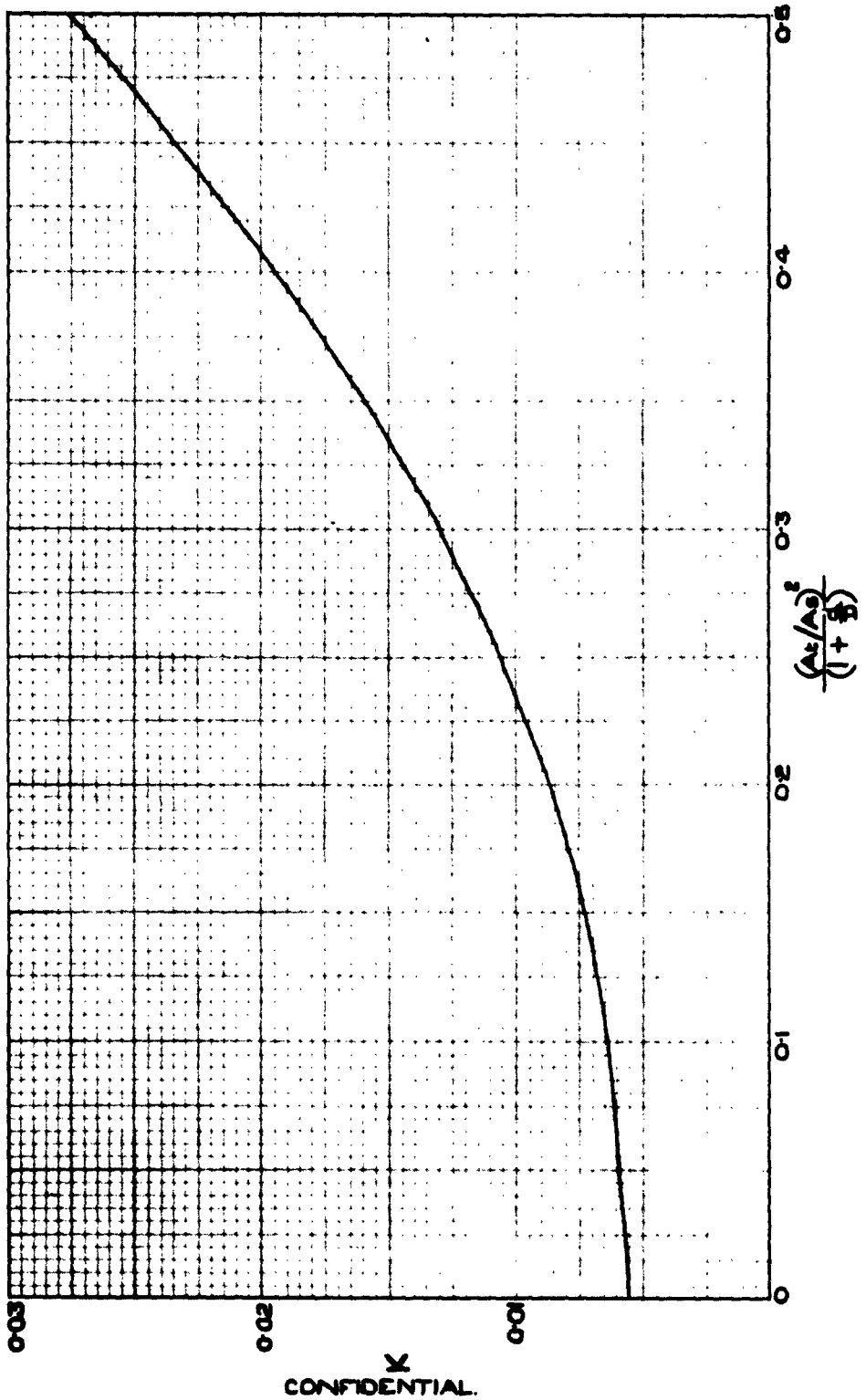

CONFIDENTIAL.

FIG.5.

EFFECT OF TRAILING EDGE THICKNESS ON BLADE LOSS COEFFICIENT.

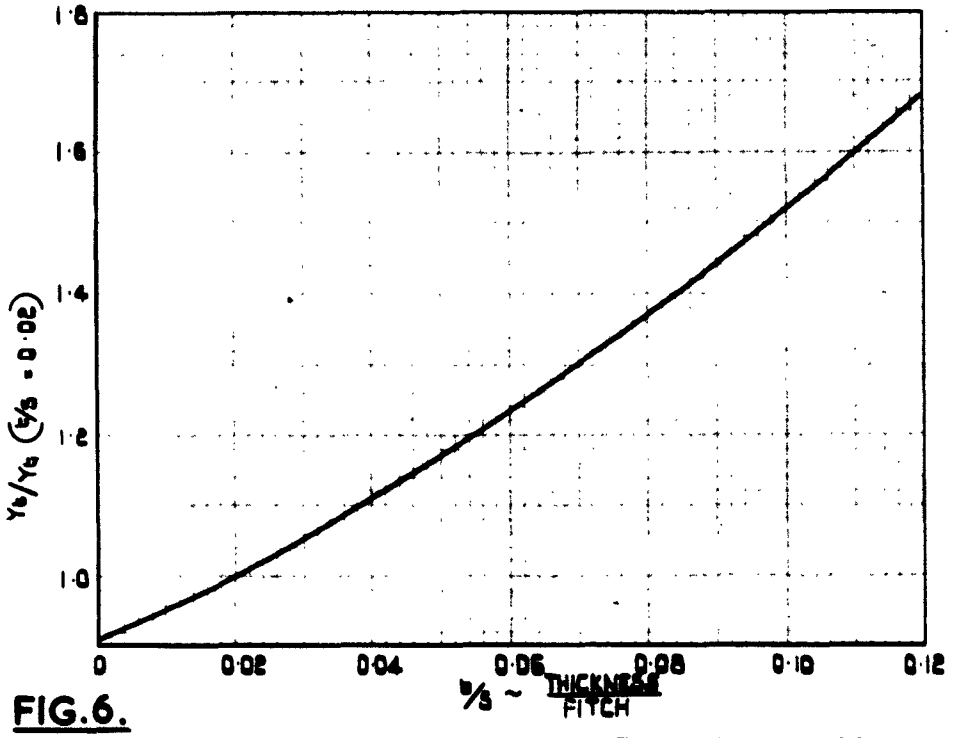

FIG.6.

VARIATION OF PROFILE LOSS WITH REYNOLDS NUMBER.

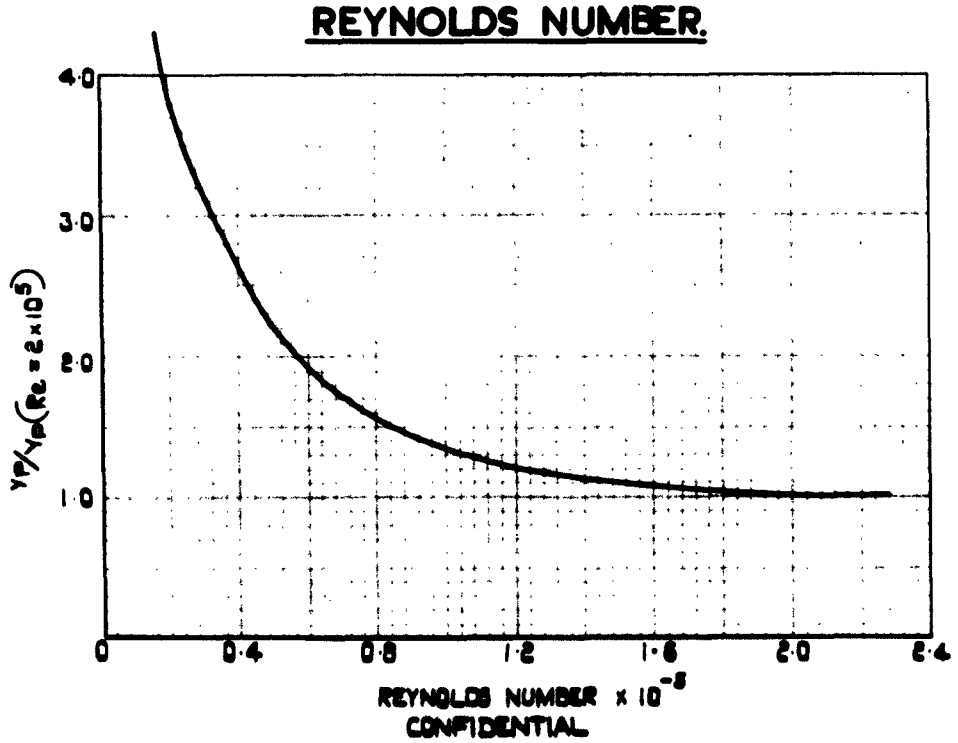

FIG. 7.

FIGS. 7, 8, & 9.

PORTED SWIRLER.

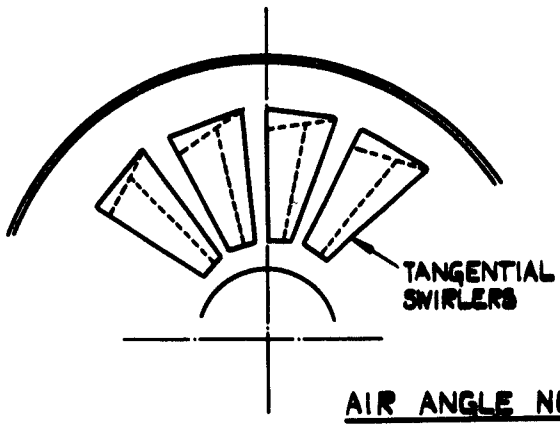

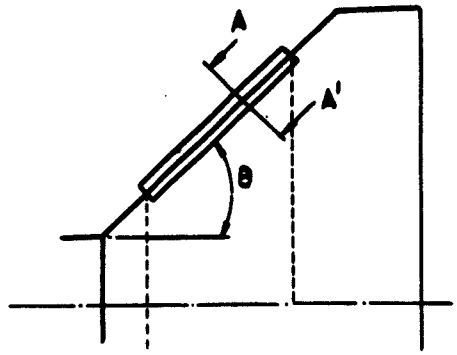

AIR ANGLE NOTATION

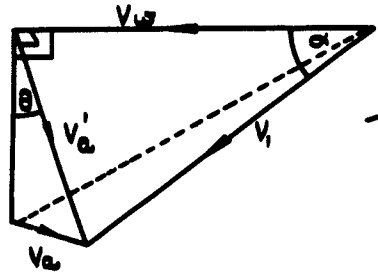

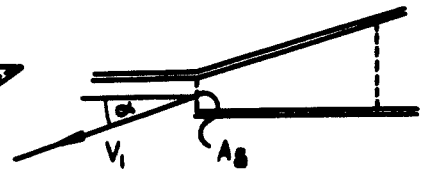

SECTION A - A'

FIG. 8.

VORTEX TYPE SWIRLER.

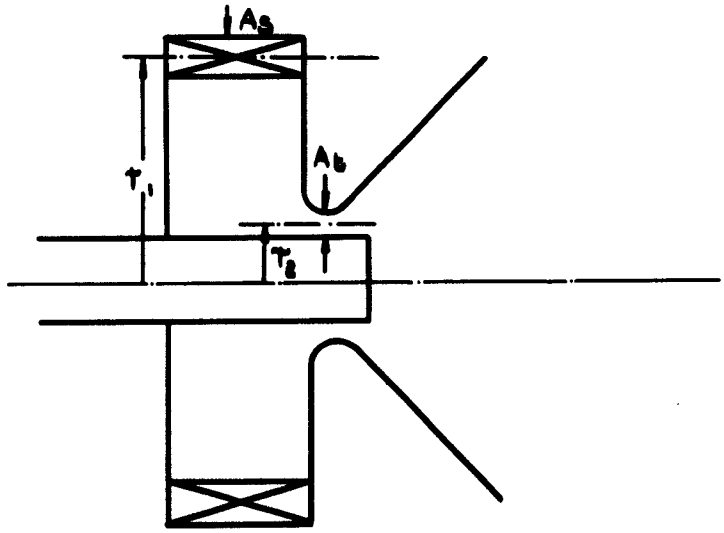

FIG. 9.

NOTATIONAL DIAGRAM (SEE 2.30.)

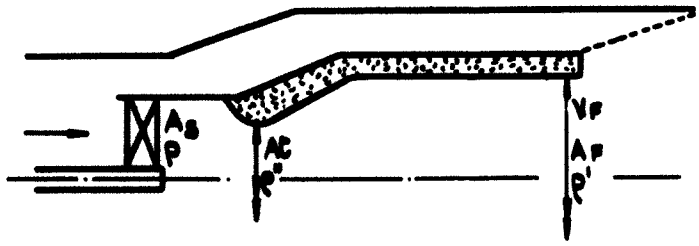

FIG.10.

VARIATION OF DISCHARGE COEFFICIENT WITH VENA CONTRACTA MACH NUMBER.

CONFIDENTIAL.

FIG. 11.

SK57577

RELATIVE DISCHARGE COEFFICIENT VERSUS AREA RATIO.

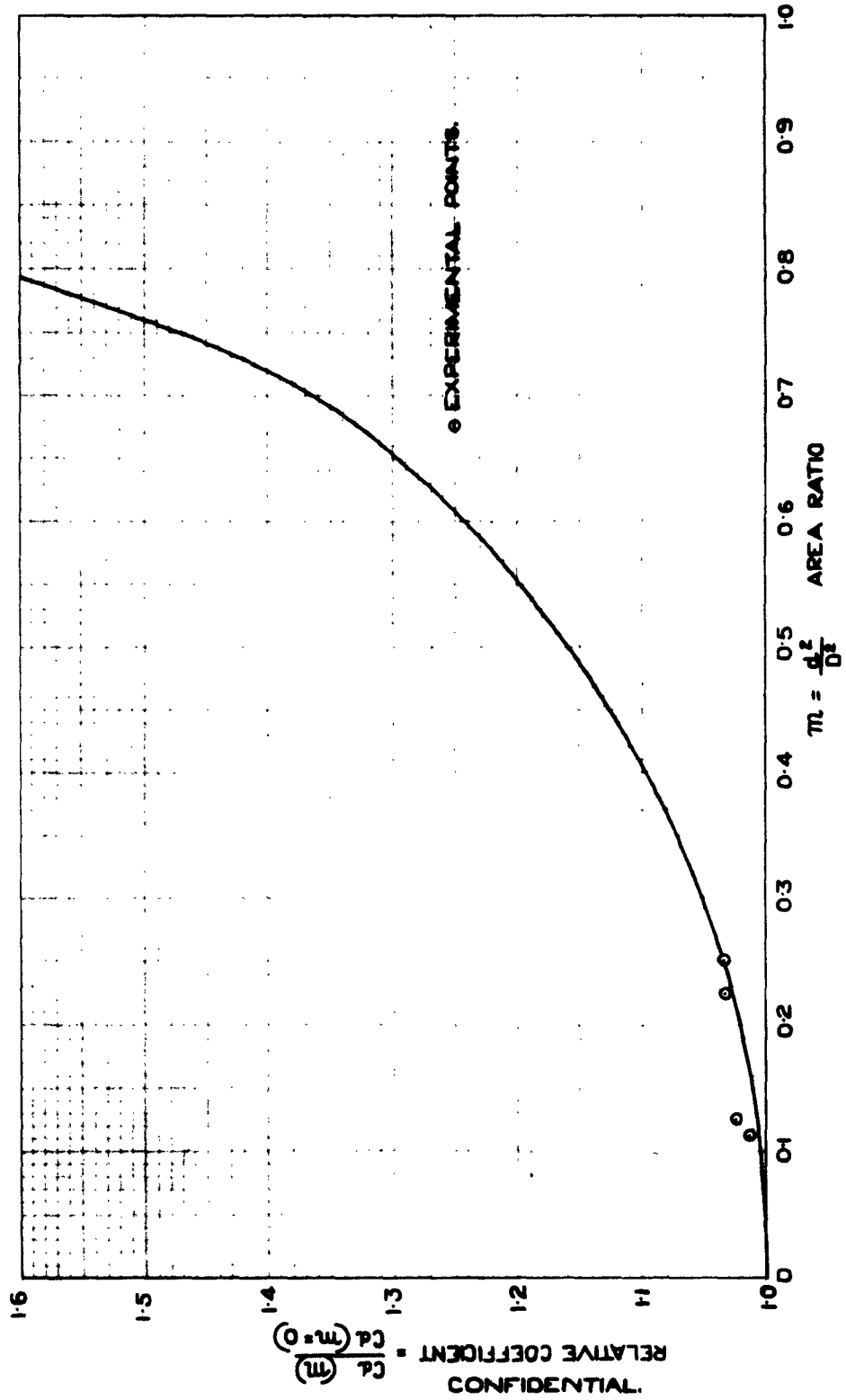

CONFIDENTIAL.

FIG. 12.

VARIATION OF LOSS COEFFICIENT WITH HOLE INCLINATION.

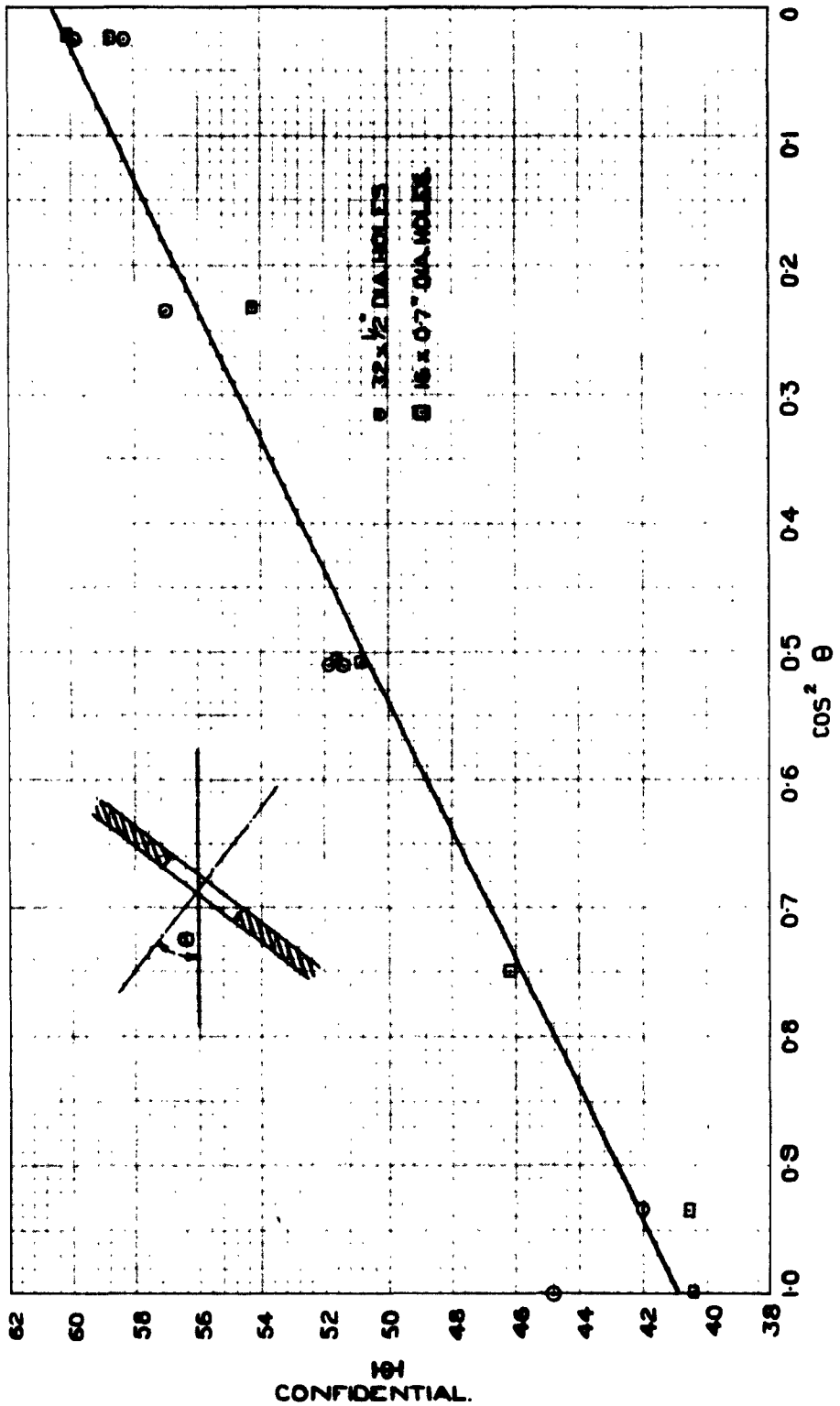

SK 5758

CONFIDENTIAL.

FIG. 13.

SK 57579

RELATIVE LOSS VERSUS HOLE INCLINATION.

FIG.14.

VARIATION OF STATIC PRESSURE DROP COEFFICIENT WITH PERCENTAGE TURBULENCE.

(FROM REF. 21)

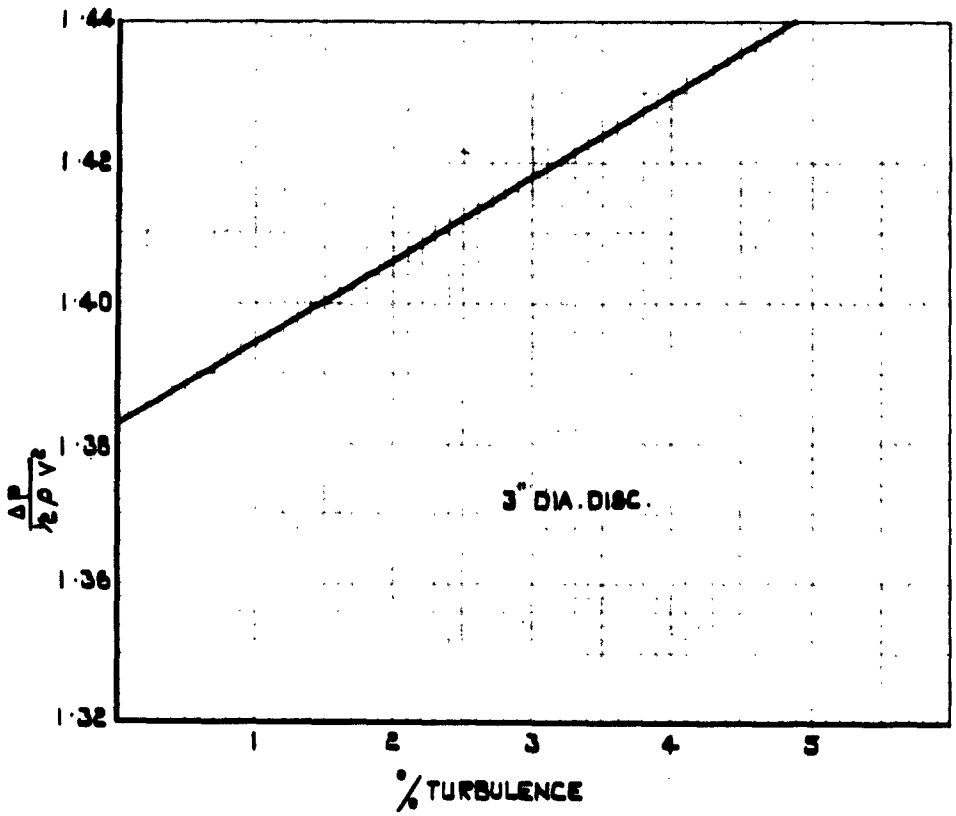

FIG.15.

FRICTION FACTOR 'f' FOR SHEET METAL SURFACES VERSUS REYNOLDS NUMBER.

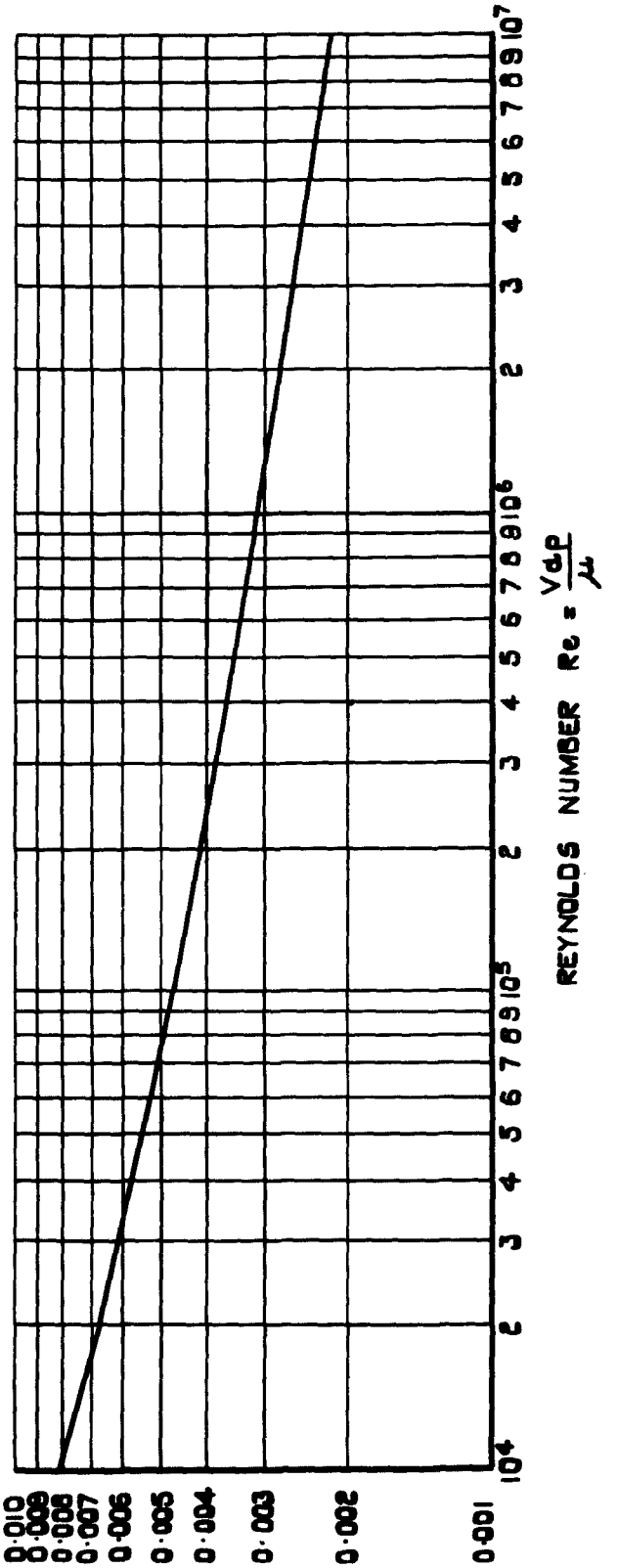

FIG.16.

GUTTER NOTATION.

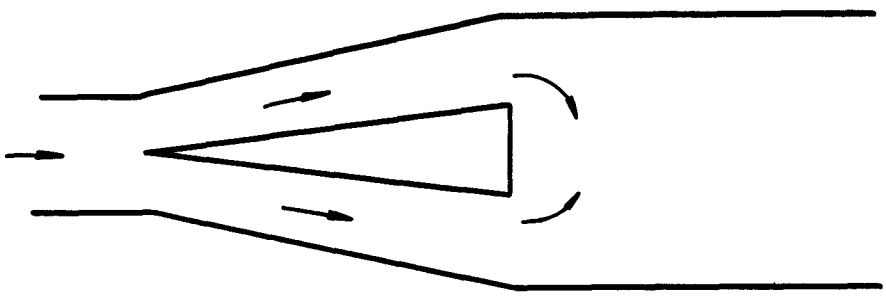

(a) CONVENTIONAL OR 'PLAIN' GUTTER.

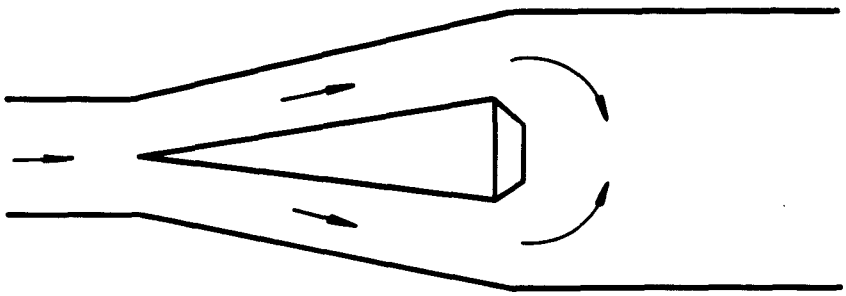

(b) 'SKIRTED' GUTTER.

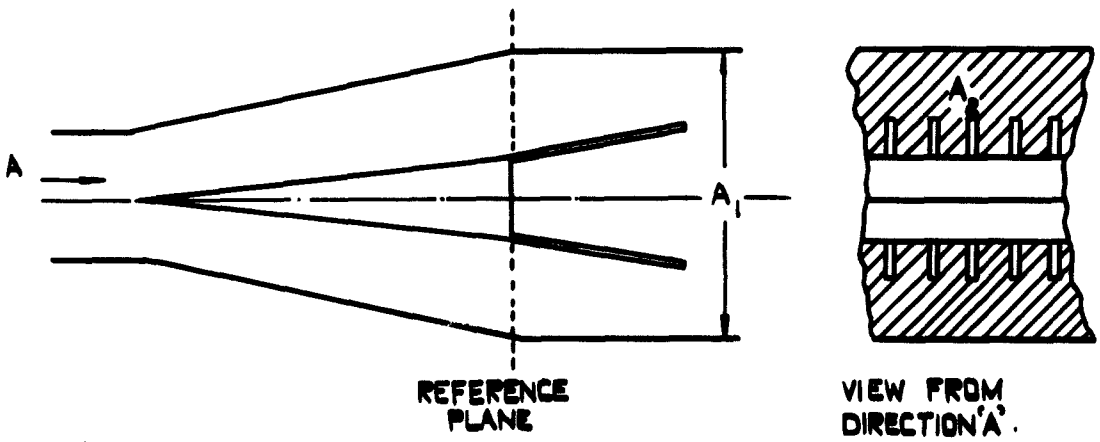

FREE AREA AT REFERENCE PLANE = A_2

AREA RATIO = $\lambda = \frac{A_1}{A_2}$

(c) NOTATION FOR 'FINGER' FLAME SPREADERS.

FIG. 17.

SK 57582.

C_d FOR HOLE IN WALL OF DUCT.

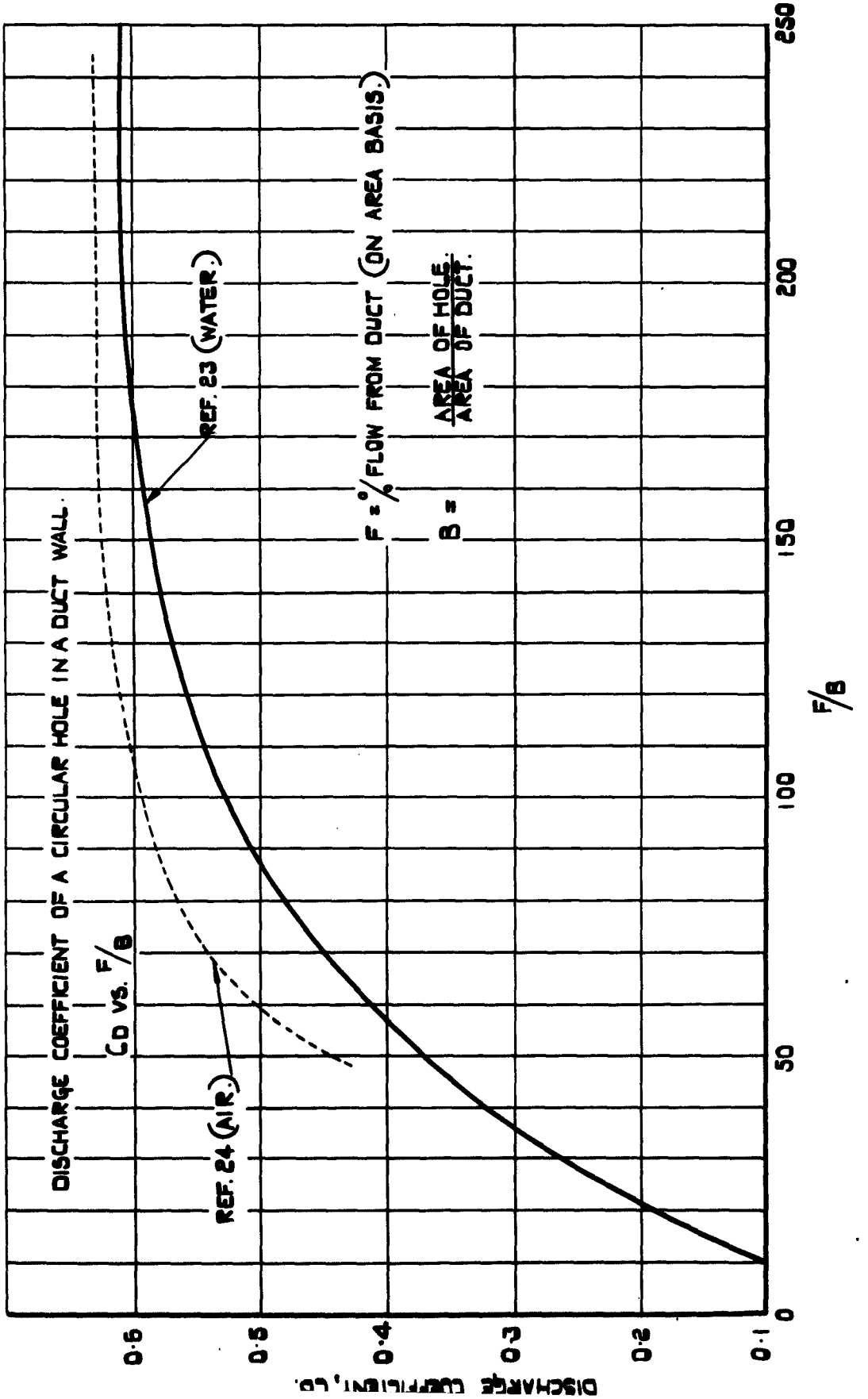

FIG. 18.

DIFFUSER EFFICIENCY (e) VERSUS DIFFUSER ANGLE (θ)

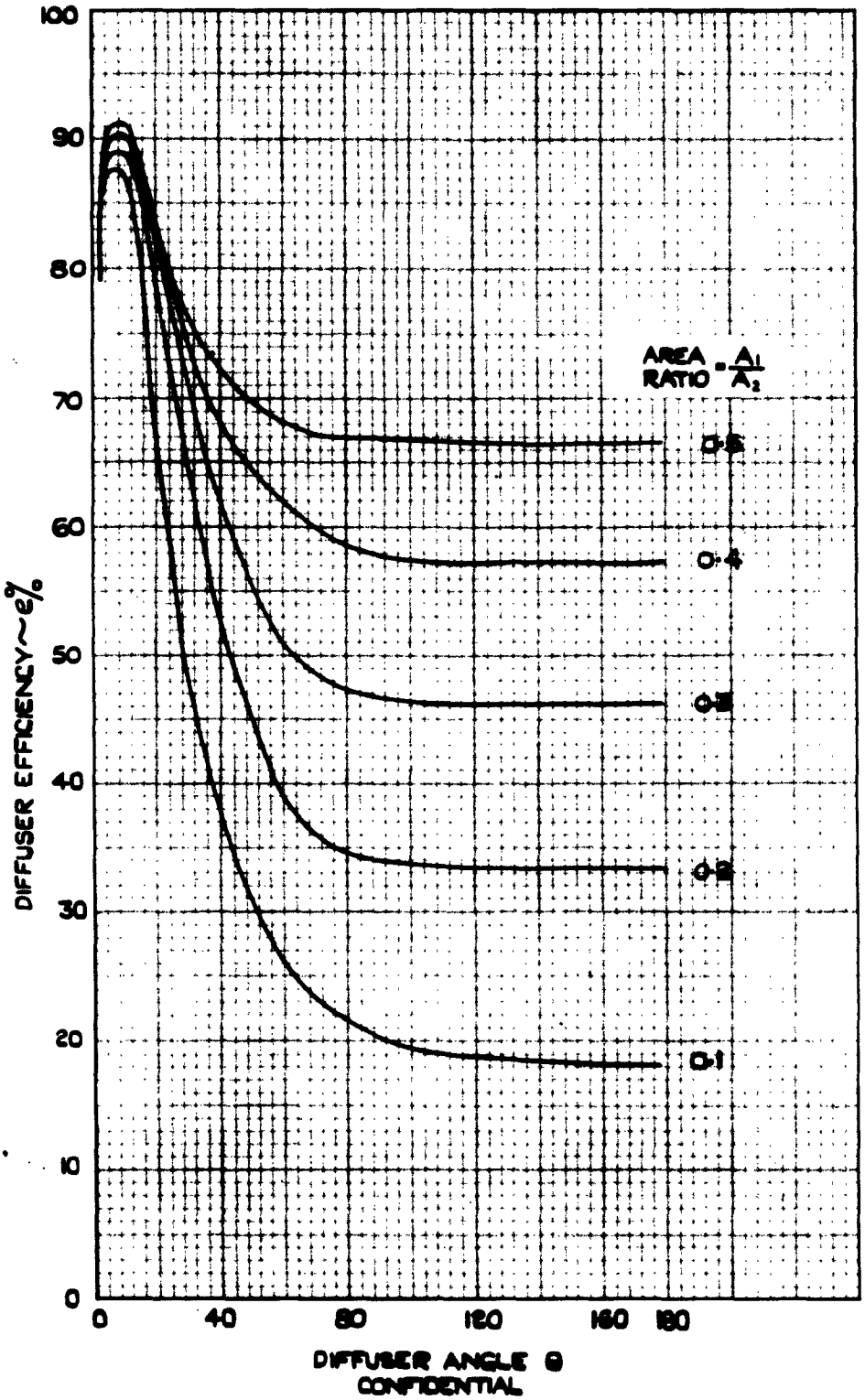

SK 57584

CONFIDENTIAL

FIG. 19.

DIAGRAM OF CONVENTIONAL COMBUSTION CHAMBER.

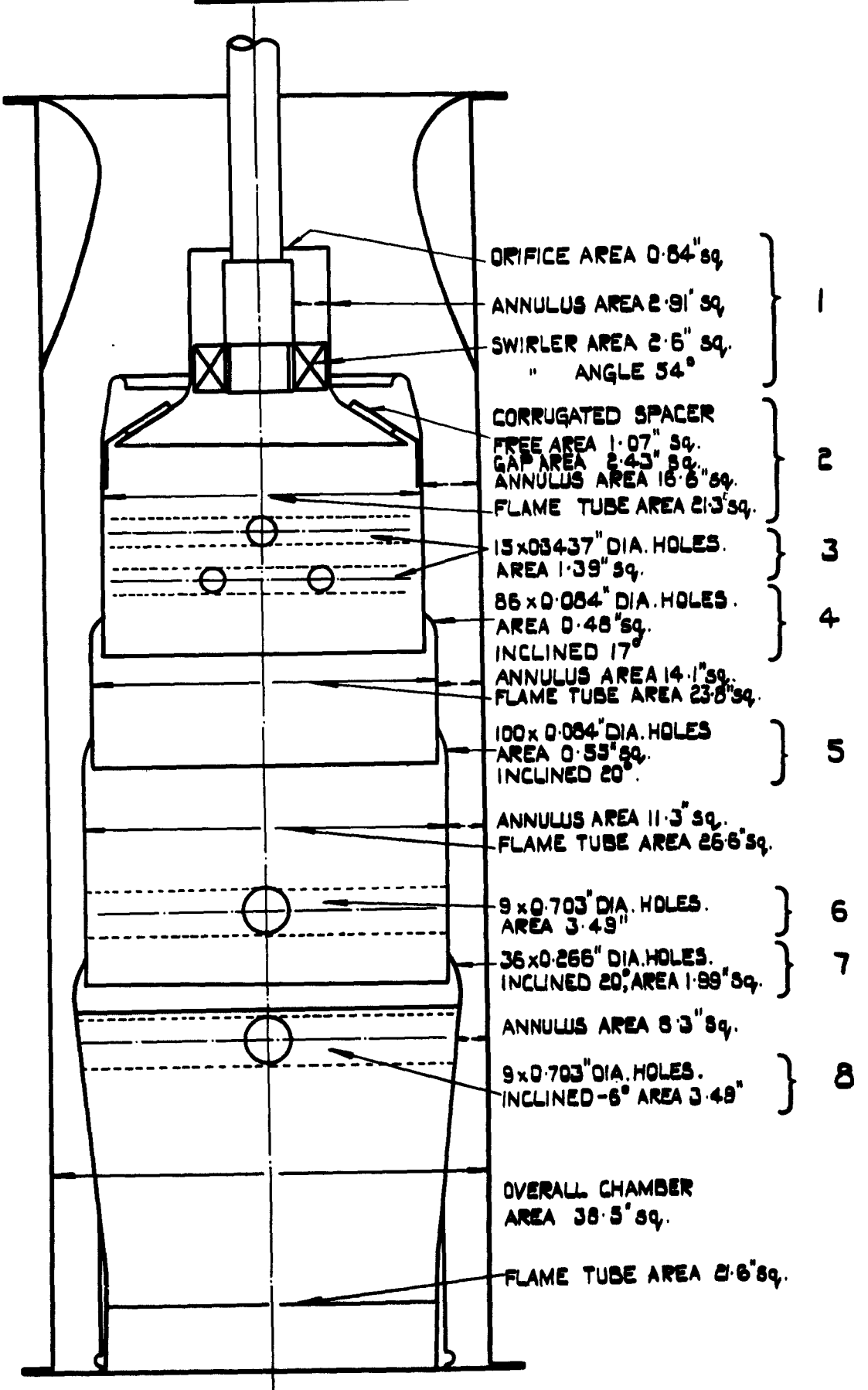

CONFIDENTIAL

Information Centre
Knowledge Services
[dstl] Porton Down,
Salisbury
Wilts
SP4 0JQ
22060-6218
Tel: 01980-613753
Fax 01980-613970

Defense Technical Information Center (DTIC)
8725 John J. Kingman Road, Suit 0944
Fort Belvoir, VA 22060-6218
U.S.A.

AD#: AD029109

Date of Search: 17 July 2008

Record Summary: AVIA 28/3689
Title: Combustion Chambers: Component Pressure Losses
Availability Open Document, Open Description, Normal Closure before FOI Act: 30 years
Former reference (Department) R143
Held by The National Archives, Kew

This document is now available at the National Archives, Kew, Surrey, United Kingdom.

DTIC has checked the National Archives Catalogue website (http://www.nationalarchives.gov.uk) and found the document is available and releasable to the public.

Access to UK public records is governed by statute, namely the Public Records Act, 1958, and the Public Records Act, 1967.
The document has been released under the 30 year rule.
(The vast majority of records selected for permanent preservation are made available to the public when they are 30 years old. This is commonly referred to as the 30 year rule and was established by the Public Records Act of 1967).

This document may be treated as UNLIMITED.